10 Sonic Boom

Lead authors

Domenic J. Maglieri
Eagle Engineering, Inc.
Hampton, Virginia

Kenneth J. Plotkin
Wyle Laboratories
Arlington, Virginia

Introduction

The introduction of the century-series fighter aircraft in the 1950's, with their ability to fly at supersonic speeds in level flight, brought into prominence the sonic boom phenomenon. This phenomenon, which is now well understood from a physical standpoint, was heretofore quite infrequent and was usually associated with aircraft which had to dive in order to attain slightly supersonic speeds. Concerted efforts in the 1960's, in conjunction with increased operations of high-performance military aircraft, the proposed (and later canceled) U.S. supersonic transport (SST), and the eventual entry of the British-French Concorde into commercial service, have provided significant insight into the generation, propagation, and prediction of sonic booms and their effects on people, animals, and structures (refs. 1 to 7). Even so, sonic booms continue to be a community acceptance problem for aircraft operations at supersonic speeds. In fact, commercial supersonic flight over land in the United States is prohibited (ref. 8). The Concorde confines its supersonic operations to overwater routes only.

Sonic boom studies continue to play a role in the formation of environmental impact statements regarding the establishment of military operational training areas and the Space Shuttle program. Recent research in long-range hypersonic vehicles, such as the "Orient Express," recognizes that the sonic boom will loom large as a serious threat to complete success.

This chapter is intended to provide a status of the knowledge of sonic booms, with emphasis on their generation, propagation, and prediction. For completeness, however, material relating to the potential for sonic boom alleviation and the response to sonic booms is also included. The material is presented in the following five sections: *Nature of Sonic Booms, Review and Status of Theory, Measurements and Predictions, Sonic Boom Minimization, and Responses to Sonic Booms.*

Nature of Sonic Booms

This section begins with a description of the shock flow fields surrounding bodies moving at supersonic speeds and the manner in which sonic booms are observed. A description of the sonic boom carpets, both primary and secondary, is given for a

typical aircraft operation. The role of the atmosphere in establishing and influencing the primary and secondary booms is discussed.

Shock Flow Field

Any body which moves through the air at speeds exceeding the local speed of sound has associated with it a system of shock waves, as shown in figure 1. A simple body of revolution (i.e., a projectile) generally has two waves, one attached to the front called the bow wave and the other emanating from the rear called the tail wave (fig. 1(a)). More complicated configurations, such as the small aircraft model in figure 1(b), produce whole systems of shock waves. At very large distances from the body, the wave system tends to distort and steepen, ultimately coalescing into a bow and a tail wave as in the case of the simple projectile.

Figure 1(c) shows a schematic diagram representing the far-field wave patterns typical of the projectile and wind-tunnel data. At the bow wave a compression occurs in which the local pressure p rises to a value Δp above atmospheric pressure. Then a slow expansion occurs until some value below atmospheric pressure is reached, after which there is a sudden recompression at the tail wave. Generally, the bow and tail shocks are of similar strengths and the pressure decreases linearly between the two. This nominal sonic boom signature is called an N-wave. It moves with the aircraft and is associated with continuous supersonic flight, not just with "breaking the sound barrier." One speaks of a sonic boom "carpet," whose width depends on flight and atmospheric conditions, swept out under the full length of a supersonic flight. Receivers within the carpet detect the sonic boom—that is, the N-wave—once as the aircraft passes.

If these waves were sweeping by an observer on the ground, the ear's aural response would be as shown schematically in the sketch at the bottom of figure 1(c). Since the ear detects changes in pressure only above a certain frequency, it would respond to the steep part of the wave and not to the portion which is changing slowly. If the time interval Δt between those two rapid compressions is small, as for a bullet, the ear would not be able to distinguish between them and they would seem as one explosive sound. If the time interval is on the order of 0.10 sec or greater, as is the case for an aircraft at high altitude, the ear would probably detect two booms.

Some of the characteristics of the pressure signatures within the flow field surrounding the XB-70 aircraft are shown in figure 2. These in-flight measurements (ref. 9) were obtained by probing the flow field above and below the XB-70 with an instrumented aircraft. The XB-70 was flying at $M = 1.5$ at 37 000 ft above ground level, and in-flight surveys were made at 2000 ft above and at 2000 and 5000 ft below the aircraft. Also shown is the corresponding signature measured at ground level.

The measured signatures are shaded to highlight the individual pressure peaks. These pressure peaks are associated with details of the aircraft geometry (wings, inlets, canopy, empennage, and so on). It is shown that more complex signatures are measured close to the aircraft and that the individual shock waves from the aircraft tend to coalesce as distance from the aircraft increases, although in this case an ideal N-wave has not yet evolved. It is also shown that the shock wave signature above the aircraft differs markedly (in shape and amplitude) from that below the aircraft at a comparable distance. This signature difference results from the difference in the detailed geometry of the aircraft and the manner in which the volume and lift components interact.

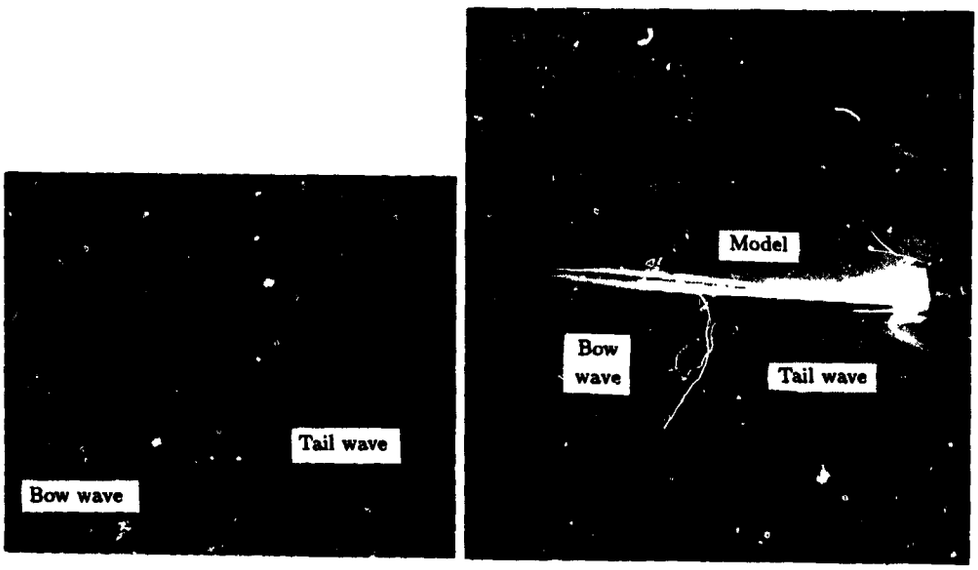

(a) Flow field for projectile. *(b) Flow field for aircraft.*

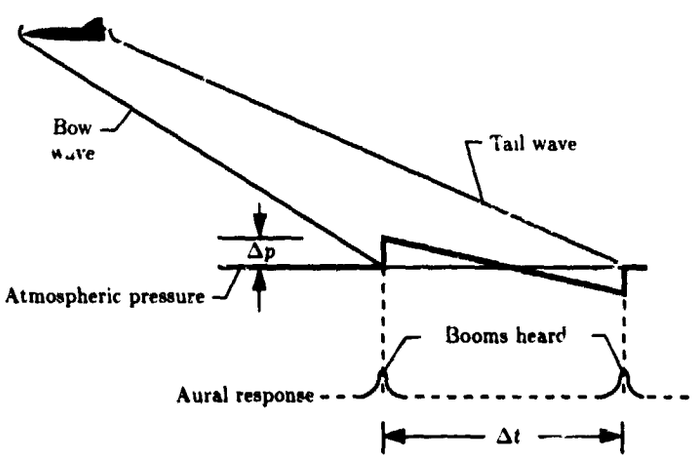

(c) Far-field wave patterns.

Figure 1. Shock flow fields.

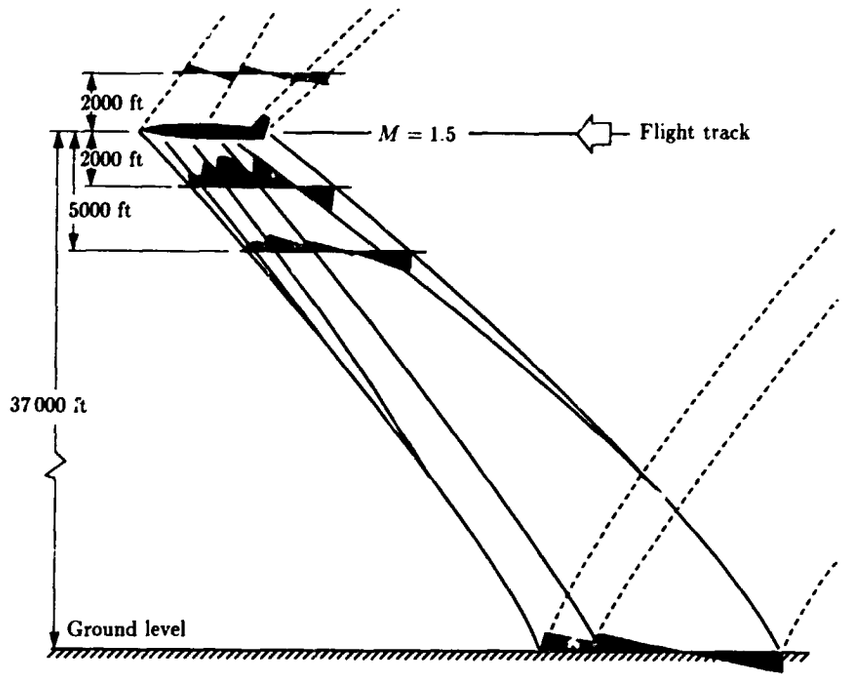

Figure 2. Measured signatures above and below XB-70 aircraft.

Description of Sonic Boom Carpets

Figure 3 shows schematically the nature of the sonic boom carpets for a flight such as that of the Concorde, during which the aircraft flies a large portion of the distance supersonically and without maneuvers. Two ground exposure patterns in which booms are observed are shown. The primary boom carpet contains the normally observed sonic boom overpressures and results from wave propagation through only that part of the atmosphere below the aircraft. Secondary boom carpets may exist which involve the portion of the atmosphere above the aircraft as well as that below the aircraft. Between the primary and secondary carpets exists a region in which no sonic booms are observed. The secondary boom carpets are more remote from the ground track and the overpressure levels are much less intense than in the primary carpet.

The waveform characteristics of the boom signatures can vary widely at the different observation points, as indicated in figure 3. In the region of the primary boom carpet, on or near the ground track, N-wave signatures are typically observed. For typical high-altitude cruise conditions, these are usually of the order of 1 to 3 lb/ft^2 in intensity and from 0.10 to 0.30 sec in duration. At the fringes of the primary boom carpet, near the lateral cutoff, the signatures degenerate into weak sound waves and they lose their N-wave characteristics. In the region of the secondary boom carpet, the disturbances tend to be very weak in intensity (of the order of 0.02 to 0.20 lb/ft^2) but persist over longer periods of time (refs. 10 to 15).

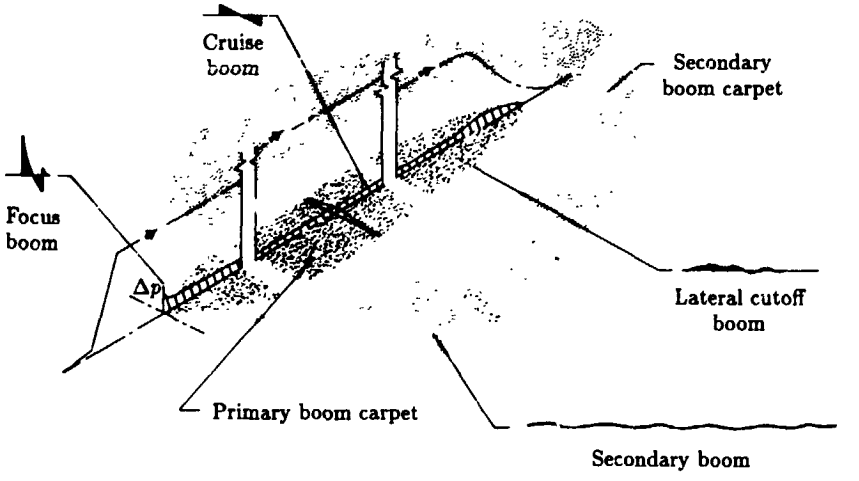

Figure 3. Nature and extent of sonic boom ground exposure carpets and waveforms associated with supersonic aircraft operations.

It should be noted that the higher overpressure N-wave sonic booms have caused community acceptance problems. On the other hand, the lateral cutoff booms and the secondary booms, which do not have an N-wave character and are lower in intensity, tend to be more of a curiosity and are not apt to be the source of serious community response problems. Near the lateral cutoff, primary booms usually resemble low rumbles or rolling thunder. Secondary booms, however, are generally not audible (0.1 to 1.0 Hz), but can cause building vibrations which are readily observed.

Another type of pressure signature, that of a focus boom (shown in the lower left of fig. 3), can be observed when any aircraft accelerates from subsonic to supersonic speeds. These "acceleration" focus booms are followed by regions on the ground in which multiple booms are observed. The focus booms enhance the booms generated in steady, level flight operations.

Sonic boom footprints from military operations, particularly air combat maneuvers, can be quite complex. They have the same essential features as shown in figure 3, but can have a very short cruise component (because of the brief nature of supersonic combat maneuvers) and can be distorted by turns.

Role of the Atmosphere

The manner in which the atmosphere above and below the aircraft is involved in developing the primary and secondary boom carpets is shown in more detail in the ray diagram of figure 4. On the right-hand side of figure 4 are examples of temperature and wind profiles for a normal atmosphere. Of note is that there is a portion of the higher atmosphere in which the temperature increases as altitude increases, and the associated wave propagation speed thus increases compared with that in the lower portions of the atmosphere. Similarly, the wind may participate in such a way as to further increase the wave propagation speed in certain directions.

On the left-hand side of figure 4 is a ray diagram for an aircraft at an altitude of 60 000 ft, traveling toward the viewer. The downward-propagating rays, shown by the solid lines, impact the ground to form the primary carpet, as indicated in

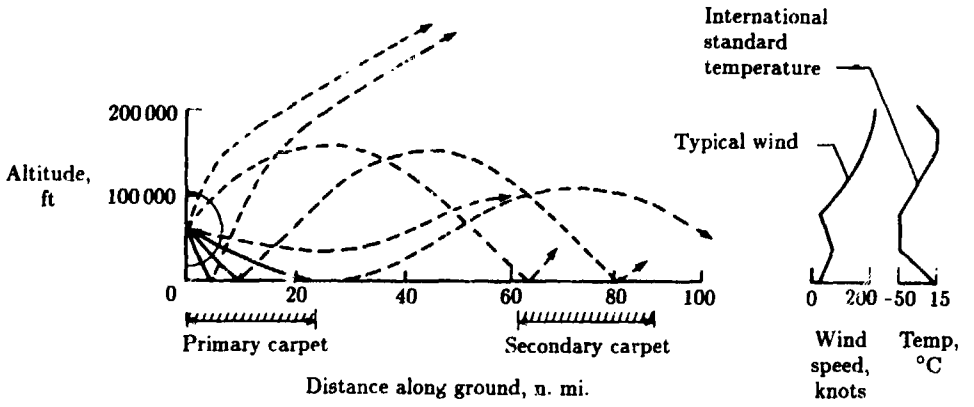

Figure 4. Propagation paths of sonic boom disturbances from an aircraft and associated ground exposure carpets.

the figure. At some point—about 28 n.mi. in the example shown—the rays refract away from the ground and thus define the lateral extent of the primary carpet. Also indicated is a secondary carpet, at about 65 to 85 n.mi. from the flight track, in which the dashed-line rays impact. These dashed-line rays arrive in two different ways: they either travel directly to the secondary carpet as a result of bending in the upper atmosphere, or they may first impinge in the primary carpet, reflect upward from the surface, and then bend downward after traveling through a portion of the upper atmosphere. The representation of the secondary carpet in this illustration is probably oversimplified, because there is reason to believe that it could consist of several well-defined impact areas (refs. 12 and 13). Variations in atmospheric wind and temperature profiles, however, could cause these impact areas to lose their identities. Some of the steep-angle rays above the aircraft may travel in such a way that they are dissipated without ever approaching the ground.

The atmosphere, particularly the first few thousand feet of the Earth's boundary layer, plays another very significant role relative to the sonic boom signature waveforms. Figure 5 presents examples of sonic boom waveforms that were measured in the primary carpet for three different types of aircraft. The tracings of measured waveforms for the F-104 aircraft are for a time duration of about 0.10 sec. The waveforms vary from the nominal N-wave shape previously described, varying from a sharply peaked to a gently rounded shape. Similar tracings are shown for the B-58 and XB-70 aircraft. The B-58 signatures are roughly 0.20 sec in duration and the XB-70 signatures are approximately 0.30 sec in duration. The main differences between waves for a given aircraft occur at the time of the rapid compressions. The largest overpressures are generally associated with the sharply peaked waves. Such differences in the sonic boom waveform result primarily from the turbulence and the thermal activities in the lower layer of the atmosphere (ref. 9).

Review and Status of Theory

In this section the theory is developed, beginning with the acoustic source and including atmospheric effects and nonlinear steepening. Sonic boom computations are sufficiently complex to necessitate computerization. A discussion of a number of

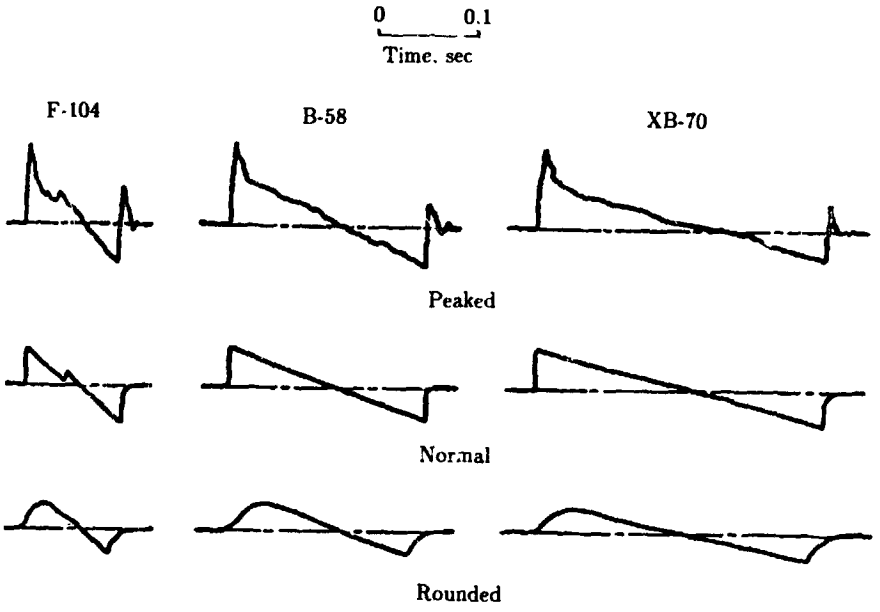

Figure 5. Variation of measured sonic boom waveforms at ground level for small, medium, and large aircraft in steady, level flight.

these programs is presented. Maneuvering flight and the potential for sonic boom focusing is addressed, along with the different types of focus conditions that may be encountered. Finally, a discussion of the applicability of the theory to hypersonic speeds is presented.

Sonic Boom Theory

A slender axisymmetric body in uniform supersonic flow, as shown in figure 1(a), generates a cylindrical acoustic wave field with overpressures $\Delta p = p - p_0$ given by

$$\Delta p(x - \beta r, r) = p_0 \frac{\gamma M^2 F(x - \beta r)}{(2\beta r)^{1/2}} \tag{1}$$

where

p	pressure
p_0	undisturbed ambient pressure
x	axial coordinate (body fixed)
r	radius
γ	ratio of specific heats
M	Mach number
β	Prandtl-Glauert factor, $\sqrt{M^2 - 1}$

and

$$F(x) = \frac{1}{2\pi} \int_0^x \frac{A''(\xi)}{(x - \xi)^{1/2}} \, d\xi \tag{2}$$

where A is the cross-sectional area of the body as measured by cutting planes aligned with the Mach angle and ξ is a dummy variable of integration. The quantity $F(x)$ was introduced by Whitham (ref. 16) and is generally referred to as the Whitham F-function. The F-function has an implicit dependence on Mach number because of A being defined on Mach tangent cutting planes, so that, in principle, Mach number dependence is not limited to the explicit factors in equation (2). In practice, the Mach number dependence of equation (2) is relatively weak, so an F-function computed at one Mach number can be considered to be "the" F-function over a reasonable range of conditions.

Equations (1) and (2) are derived from linearized supersonic flow and area-rule theory for axisymmetric bodies. They can be shown to be valid for nonaxisymmetric vehicles if the actual area $A(x)$ is replaced with an equivalent area which is a function of azimuthal angle about an axis through the body in the flight direction. The equivalent area consists of two components: the actual area as cut by a plane tangent to the Mach cone at the azimuth plus an effective area directly proportional to the axial distribution of lift in that direction. This formulation follows from the linearized supersonic flow and area-rule results of Hayes (refs. 17 and 18) and Lomax (ref. 19) and was applied by Walkden (ref. 20) to Whitham's basic sonic boom analysis (ref. 21, discussed below), leading to the analysis of sonic booms in terms of volume and lift components. When generalized to asymmetric bodies, the locally asymmetric version of equation (1) is valid at distances which are large compared with body dimensions (i.e., $r \gg x - \beta r$). A very good presentation of the equivalent area formulation is given in reference 22, which also contains a more detailed presentation of sonic boom theory than the current synopsis.

The complete role of the aircraft configuration in sonic boom generation is embodied in the F-function. Analysis of minimization concepts generally centers on calculating F-functions for various configurations. At hypersonic speeds, for which linearized flow theory is not accurate, the problem is that of obtaining the F-function by means other than equation (2); equation (1) is always valid beyond some radius r at which $\Delta p/p_0$ is sufficiently small. These two topics are discussed in detail subsequently. For now, it suffices to note that the aircraft source is defined by the F-function.

Pressure signatures at large distances do not retain the fixed shape of equations (1) and (2); explosions and supersonic artillery projectiles were long known to generate far-field shock wave signatures. Landau (ref. 23) showed that weak nonlinear effects (second order in overpressure) cause the far-field signature of a projectile to have a dual-shock N-wave shape. The mechanism is that air in the positive-pressure pulse has an elevated temperature and a forward velocity, so that local propagation speed is faster than ambient sound speed and the wave steepens, eventually forming a shock. Landau obtained the result that shock strength in the axisymmetric case follows an $r^{-3/4}$ law rather than the $r^{-1/2}$ law of equation (1). DuMond et al. (ref. 24) performed a series of measurements on small-caliber projectiles, clearly demonstrating the N-wave and the $r^{-3/4}$ law.

The theory supporting this mechanism was set forth in a consistent manner by Whitham (refs. 16 and 21) who showed that second-order nonlinear steepening could be viewed as a uniform first-order solution: the linear solution (eq. (1)) provides the correct amplitude to the first order, but the location ($x-\beta r$, representing propagation

at the ambient sound speed) is correct only to the zeroth order. Correcting propagation speed to the first order (based on the linear solution) provides the required second-order solution.

In the form used by Whitham (ref. 21), the acoustic overpressure may be written as

$$\frac{p - p_0}{p_0} = \frac{F(\tau)}{\sqrt{S}} \tag{3}$$

where

τ	$t - (s/c_0)$
t	time
s	distance along a ray
S	ray-tube area
c_0	undisturbed ambient sound speed

where a ray-fixed coordinate system has been adopted. Figure 6 shows the relation between a wave-fixed viewpoint, as shown in figures 1 and 2, and a ray-fixed viewpoint, as sketched in figure 4. The wave front exists at a given time, whereas the rays represent the path that the boom will take after being generated at some time. The ray-tube area term $1/\sqrt{S}$ is a generalization of the cylindrical wave quantity $\gamma M^2/(2\beta r)^{1/2}$ in equation (1). For plane waves S is a constant, and for spherical waves it is proportional to r^2 or s^2. In a general nonuniform atmosphere, an acoustic impedance factor is present and S is the geometrical acoustic ray-tube area (to be discussed subsequently).

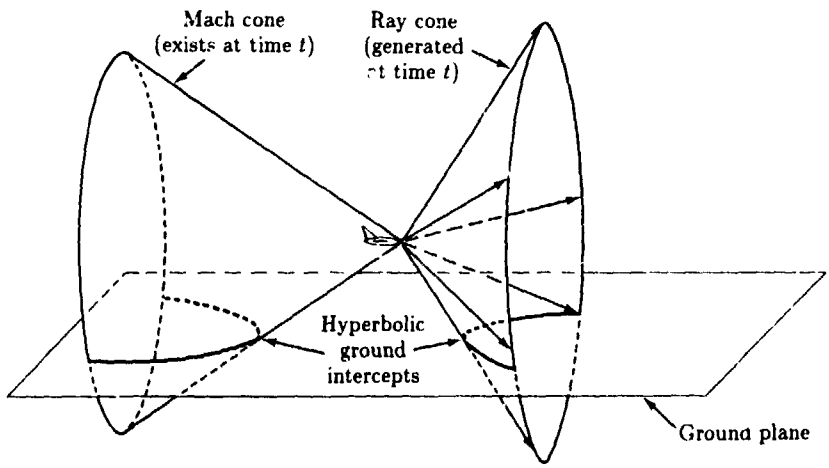

Figure 6. Mach and ray cones in supersonic flight.

Whitham's rule calls for replacing c_0 in τ by $c + u$, the perturbed sound speed c plus the velocity perturbation u. The normalized perturbations $(c - c_0)/c_0$ and u/c_0 are both proportional to $(p - p_0)/p_0$. For an isentropic acoustic wave, the propagation speed is

$$c + u = c_0 \left(1 + \frac{\gamma + 1}{2\gamma} \frac{p - p_0}{p_0}\right) \tag{4}$$

The parameter τ represents a point on the acoustic wave, and t is its arrival time at location s. The arrival time may be obtained by integrating the reciprocal of equation (4). To the first order in $\Delta p/p_0$, this arrival time is

$$t = \tau + \frac{s}{c_0} - \frac{\gamma+1}{2\gamma c_0} F(\tau) \int_0^s \frac{ds}{\sqrt{S}} \tag{5}$$

Equation (5) has been written in terms of t, rather than τ, to present an explicit relationship.

The physical interpretation of equations (3) and (5) is illustrated in figure 7. A signature near the aircraft (fig. 7(a)) undergoes an amplitude change because of the ray-tube area factor (fig. 7(b)) and undergoes a steepening distortion (fig. 7(c)) as given by equation (5). One point in the signature is highlighted in the figure and traced through this process. Note that the advance of each signature point (the last term of eq. (5)) is proportional to its F-function value and a quadrature which is independent of F. The quadrature term is part of the ray geometry solution and, in various normalized forms, has been denoted as the age parameter (ref. 25) or the advance factor (ref. 26).

Parts of the aged signature constructed in figure 7 are triple valued. This is physically impossible. At some earlier time the aging process would have caused the signature slope to be vertical, at which point there would be a discontinuous pressure jump. Propagation of this jump must be handled as a shock wave rather than as an isentropic wave. Linearizing the Rankine-Hugoniot relations gives the following speed u_s for a weak shock of strength Δp:

$$u_s \simeq c_0 \left(1 + \frac{\gamma+1}{4\gamma} \frac{\Delta p}{p_0}\right) \tag{6}$$

This is slower than the isentropic wave speed behind it, so that the original signature is absorbed into the shock. The shock is sketched in figure 7(c). In general, the linearized shock speed is equal to the average of the isentropic wave speeds ahead of and behind the shock. This leads to the "area balancing" rule for fitting shocks: construct the steepened isentropic signature, then eliminate triple-valued areas by fitting shocks such that total area is conserved. In figure 7(c), the shaded areas ahead of and behind the shock are equal.

Figure 7(c) is similar to sketches by Landau (ref. 23) and Whitham (ref. 21) showing the evolution of an N-wave signature. Key quantities for an N-wave are the shock overpressure and the total duration. Concentrating on the forward, positive-overpressure portion of the N-wave, they matched equations (3), (5), and (6) to obtain a closed-form solution.

Whitham's final result for the far-field bow shock overpressure is

$$\Delta p_{\text{shock}} \approx \frac{p_0}{S} \left[2 \int_0^{\tau_0} F(\tau)\, d\tau\right]^{1/2} \left(\frac{\gamma+1}{2\gamma c_0} \int_0^s \frac{ds}{\sqrt{S}}\right)^{1/2} \tag{7}$$

where τ_0 is the value of τ corresponding to the end of the positive phase of the F-function. For a uniform atmosphere, where $S \propto r \propto s$, equation (7) reduces to an $r^{-3/4}$ law. A similar result for the duration of an N-wave follows an $r^{1/4}$ law.

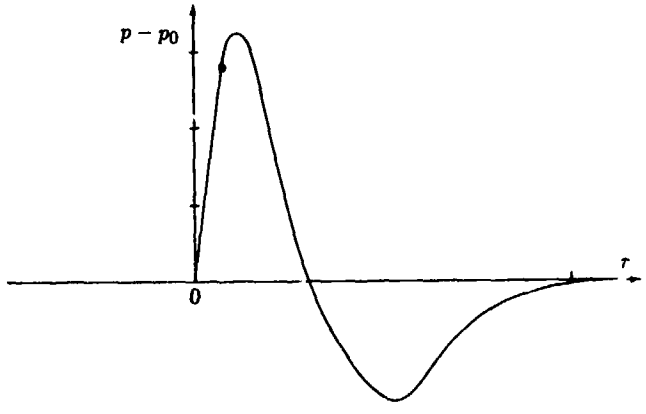

(a) Signature near aircraft (F-function shape).

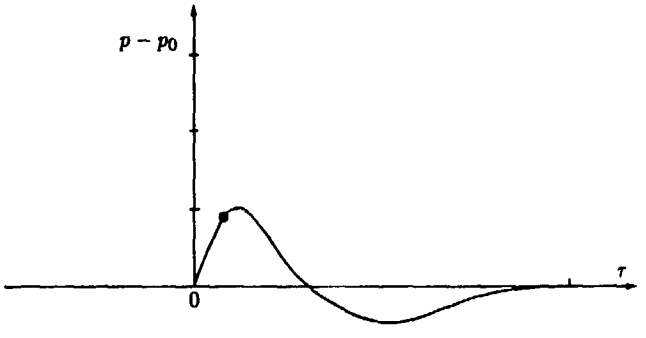

(b) Far-field acoustic amplitude change (F-function shape).

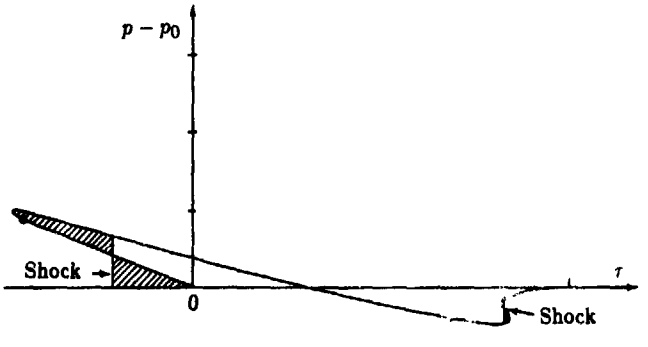

(c) Far-field steepened (aged) signature.

Figure 7. Evolution and steepening of sonic boom signature.

Equation (7) is very simple; it contains terms related to the ray-tube area dependence of the acoustic overpressure, with the aircraft geometry embodied in a simple integral of the F-function. This suggests that a far-field sonic boom is not particularly sensitive to fine details of the aircraft, and flight test results indeed show that N-waves for various conventionally shaped aircraft of similar size and weight are virtually the same. In this N-wave regime, the effect of size is that boom overpressures decrease as a function of the aircraft length to the one-fourth power. Lift-induced boom varies as the square root of aircraft weight, and the boom is relatively insensitive to Mach number.

Early calculations of sonic booms exploited this behavior. One expression used for volume-induced sonic boom was (ref. 27)

$$\Delta p = K_r K_s \sqrt{P_v P_g}(M^2-1)^{1/8}\frac{D}{l^{1/4}}\,r^{-3/4} \tag{8}$$

where

K_r	ground reflection coefficient (usually 2)
K_s	aircraft shape constant, typically 0.4 to 0.8
D	equivalent aircraft diameter
l	aircraft length
P_v, P_g	ambient pressure at the vehicle and the ground

Based on the Walkden theory (ref. 20), similar formulas were developed for lift-induced sonic boom.

The $\sqrt{P_v P_g}$ factor in equation (8) is a partial adjustment for the fact that the atmosphere is not uniform. A complete adjustment for the atmosphere utilizes the theory of geometrical acoustics. This theory accounts for curvature of shock waves and rays (as in figs. 2 and 4 and compared with the straight lines of fig. 6) and the variation in sound speed and air density. A full derivation of geometrical acoustics was presented by Blokhintzev (ref. 28). Two other noteworthy derivations are those in references 29 and 30. Geometrical acoustics applies for waves which are short compared with atmospheric gradients. Ray shapes depend on sound speed and wind gradients and are computed by methods directly analogous to those of geometrical optics. Figure 8 shows typical ray curvatures for a sonic boom under standard atmospheric conditions. Figure 8(a) shows rays under the flight track. At a given time there are rays directed at various azimuthal angles ϕ, as shown in figure 8(b). A ray-tube area, as sketched in figure 8(a), is computed to account for the effect of curvature on amplitude. The effect of the ray calculation and the variation in air density and sound speed is that the quantity S in the acoustic solution (eq. (3)) is replaced with a quantity B given by

$$B = \frac{\rho_v c_v}{\rho_0 c_0}\,S \tag{9}$$

where S is the ray-tube area, $\rho_0 c_0$ is the local acoustic impedance of air, and $\rho_v c_v$ is the impedance at the vehicle. The quantity B is slightly more complex than this if there are winds.

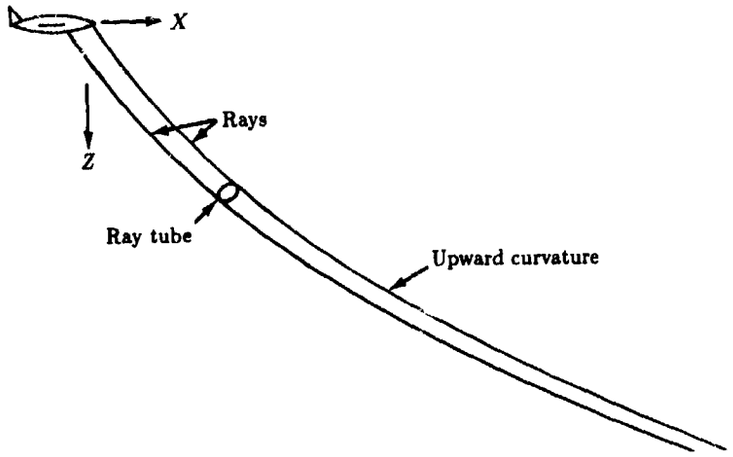

(a) Rays under flight track.

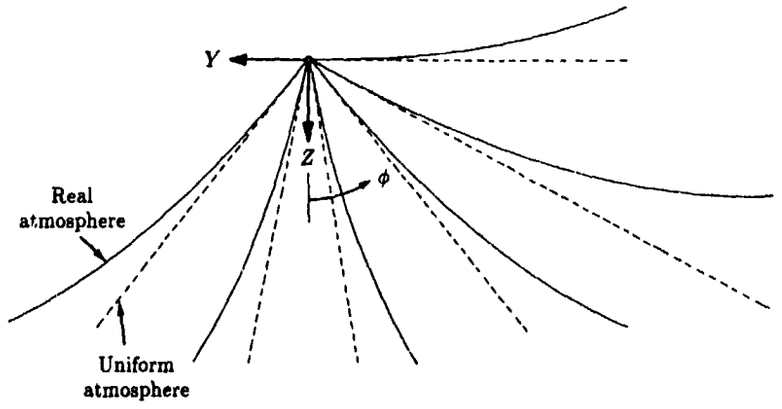

(b) Rays across flight track.

Figure 8. Curvature of sonic boom rays in atmosphere.

The ray calculation depends only on flight parameters and the atmosphere. Figure 9 shows a typical definition of four rays which outline a rectangular ray tube. Each ray lies on a ray cone. The effect of maneuvers is automatically included by use of the local flight velocity and the Mach angle at each time point. Once the ray calculation is completed, the rest of the boom calculation proceeds exactly as outlined earlier, except for the use of B instead of S throughout.

A final step in boom calculation is that, for a receiver on the ground, the perceived boom is enhanced by reflection from the ground. This reflection generally is a factor of 2. It can be less for soft ground, and it can be higher if there are multiple reflectors such as the corner between the ground and a wall.

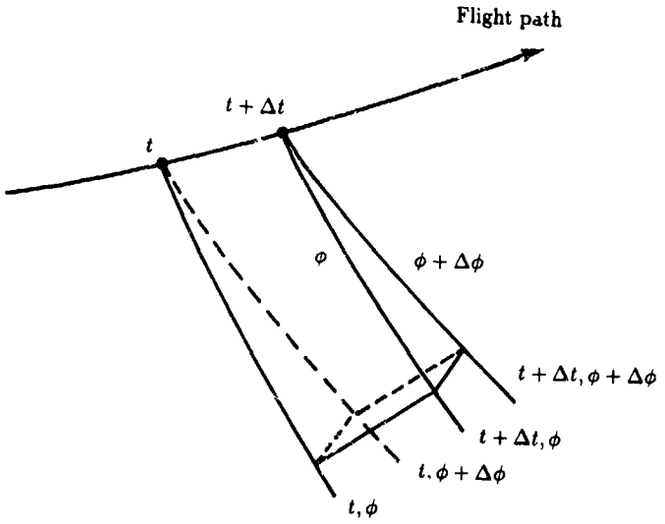

Figure 9. Ray tube outlined by four corner rays Δt and $\Delta\phi$ apart.

Computation of Sonic Booms

The theory outlined above is presented as a collection of components. The acoustic source signature is given by equations (2) and (3), with atmospheric effects included via equation (9). Nonlinear steepening is calculated by equation (5) and applied as shown in figure 7. Except for equation (8), which is very simplified, no formulas are presented by which the reader can compute sonic boom. The process is sufficiently complex that a computerized implementation is generally required. Figure 10 shows the computational flow of such a program. A number of computer programs have been written (refs. 25 and 31 to 34, for example). They all perform the same basic calculations, but each has particular capabilities and features added for specific applications. Reference 35 contains a review of the various program capabilities. All these programs were originally developed for mainframe computers. However, because of the current interest in sonic booms, it is expected that personal computer versions will be available soon.

A very useful calculation procedure for steady-flight booms is the simplified model developed by Carlson (ref. 36). He noted that the computerized geometrical acoustics calculations could be performed once for a range of flight parameters and implemented as an extension of formulas such as equation (8). His formulas for an N-wave are

$$\Delta p_{max} = K_p K_r \sqrt{P_v P_g} (M^2 - 1)^{1/8} h_e^{-3/4} l^{3/4} K_s \tag{10a}$$

$$\Delta t = K_t \frac{3.42}{c_v} \frac{M}{(M^2 - 1)^{3/8}} h_e^{1/4} l^{3/4} K_s \tag{10b}$$

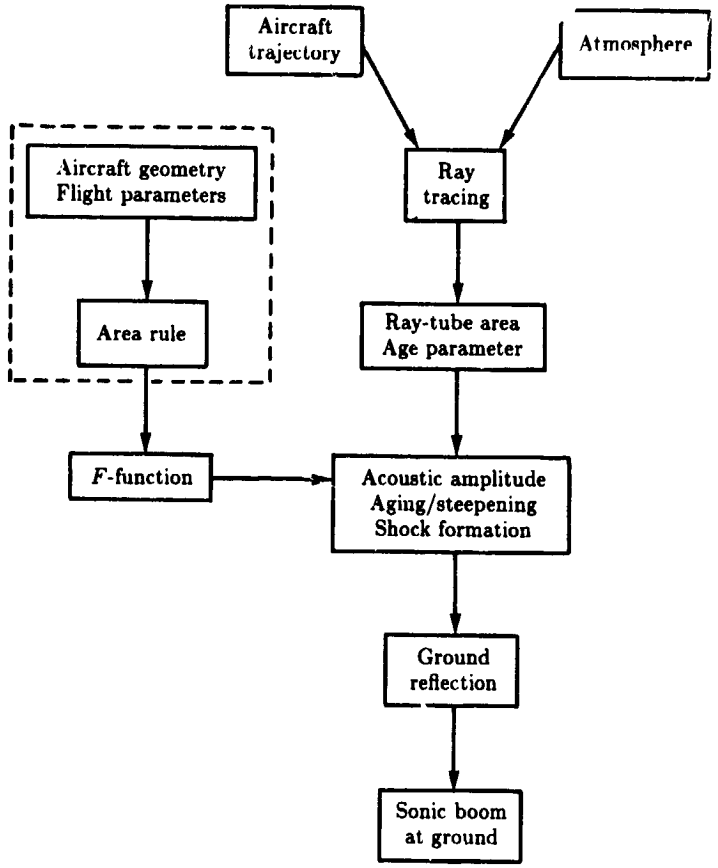

Figure 10. Logical flow of sonic boom calculation.

where

Δp_{max}	shock strength
Δt	N-wave duration
h_e	effective altitude
l	aircraft length
K_p	pressure amplification factor
K_r	ground reflection factor (nominally 2.0)
K_s	aircraft shape factor
K_t	signature duration factor

Charts of K_p and K_t are presented in reference 36 for various flight altitudes and Mach numbers. A procedure is also presented for computing K_s based on aircraft type. The K_s procedure can be used to estimate an N-wave F-function for input to a full sonic boom model with which maneuver effects can be calculated. For steady,

level flight in the standard atmosphere under conditions where N-wave sonic booms occur, Carlson's method is generally within 5 percent of computer calculations.

Maneuvers and Focusing

Under certain conditions, converging ray patterns can exist which produce focused "superbooms." Studies of cylindrical implosions and intuitive concepts of lens-like focusing give expectations of very high amplitudes. In practice, those sonic boom foci which do occur tend to be low-order types with moderate amplifications typically no more than two to five times the carpet boom shock strength.

Figure 11 illustrates a focus condition for acceleration. As the Mach number increases, the Mach angle decreases and rays converge to a focus at some distance from the aircraft. Only infinitesimally separated rays cross at a given point; the focus tends to move farther from the aircraft as M increases. The focus is thus smeared out over a line generally referred to as a caustic. There are three orders of focus to consider: a simple focus corresponding to a smooth caustic (as shown in fig. 11), a superfocus corresponding to a cusp between two smooth caustics, and a perfect lens-like focus (ref. 32). When a sonic boom focus occurs, it is predominately or completely a simple focus. Superfoci can occur for transient maneuvers such as turn entry and mark the initial point of the associated simple focus. Perfect foci do not occur for any credible supersonic maneuver.

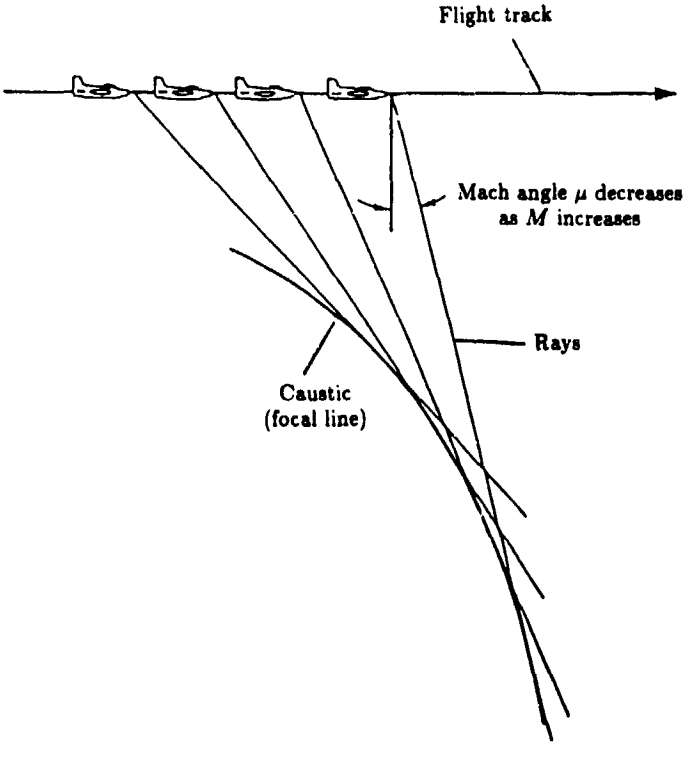

Figure 11. Sonic boom focusing due to acceleration.

In three dimensions, a caustic is a two-dimensional surface. A focal zone at the ground is a line representing the ground-caustic intersection. In three dimensions, a superfocus cusp is a line, with the superfocal zone at the ground being a point.

Figure 12 illustrates two other basic focusing maneuvers, that at sonic cutoff and that in the plane of a steady, level turn. The ray and caustic topology of these two cases and of the acceleration case of figure 11 are similar. Close to the caustic, the wave behavior depends on the relative geometry of the rays and caustics, and the three cases are mathematically interchangeable. Because the caustic represents a boundary to the wave field, the focus amplitude is limited by diffraction effects. This is a solved problem for the linear acoustic case. The linear solution is singular. The equations describing nonlinear behavior at a caustic were written by Guiraud (ref. 37), who derived a similitude and corresponding scaling law. Guiraud's scaling law leads to the following simple form for the maximum shock pressure at a simple focus:

$$\frac{p_{max}}{p_{ref}} = C\left[\frac{y_{ref}}{(\gamma+1)p_{ref}R}\right]^{1/5} \tag{11}$$

where p_{ref} is the incoming N-wave boom pressure at a normal distance y_{ref} from the caustic, R is the relative curvature between the rays and the caustic, and C is a constant. If a focused signature is available for one smooth caustic case, Guiraud's similitude can be used to adapt it to any other simple focus. The similitude also defines the size of the focal zone, within which standard boom theory is invalid. Focal zones are very narrow, with amplification significantly above the boom carpet typically within a region less than 300 ft from the focal line. Although standard boom theory can detect a focus (by virtue of ray-tube area vanishing), calculation of the focus requires that the caustic be traced and its curvature determined.

Numerical focus solutions for a single shock wave have been obtained by Gill and Seebass (ref. 38) and Gill (ref. 39) and more recently in reference 40. The Gill-Seebass solution and the scaling law have been incorporated into one of the sonic boom computer programs described previously (refs. 32 and 35). Figure 13 shows a typical focus solution for an incoming N-wave. The shocks are amplified more than the rest of the signature (typical of diffraction, which tends to wash out low frequencies more than high), so that focused signatures typically have U-shaped waves. Focus factors, based on shock amplifications, range from 2 to 5, both from calculations (ref. 41) and from flight tests (refs. 42 and 43). Calculations from this theory and flight test data are in good agreement (ref. 44).

Cusped caustic focal zones, sometimes termed "superfoci" or "super-superbooms," have been observed in flight tests (ref. 43), with shock focus factors of almost 10 at a point. Such a superfocus is limited to a region a few hundred feet in size. Theory has been formulated for cusped superfoci (refs. 45 and 46), but no results comparable to those of references 38–40 are yet available.

Hypersonic Speeds

Most parts of sonic boom theory work well at all Mach numbers, but calculation of the F-function from slender-body theory (i.e., eq. (2)) fails at high Mach numbers (above about Mach 3 for slender transport-type aircraft) or for blunt bodies. At hypersonic speeds, some other theory is required. Three approaches have been

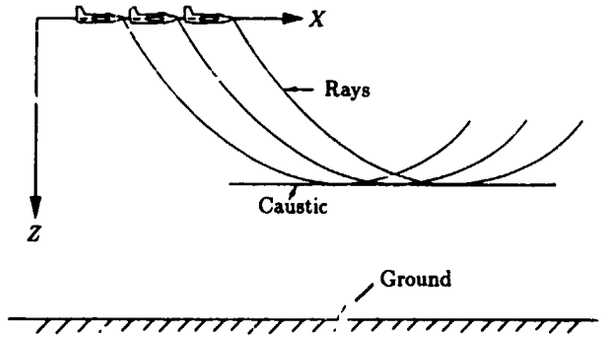

(a) Sonic cutoff.

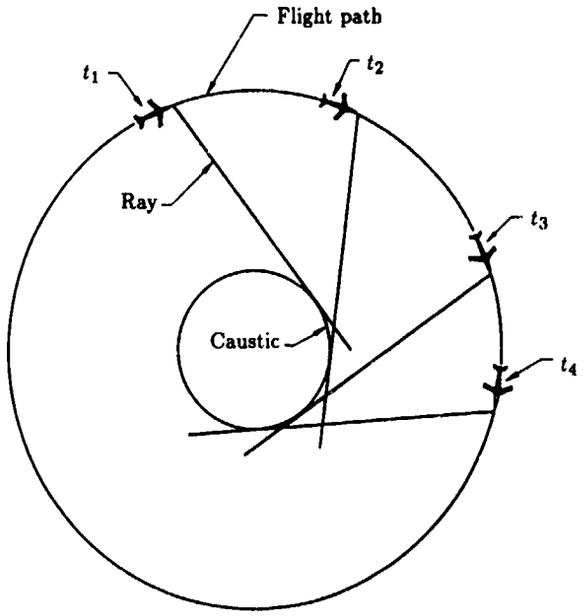

(b) Steady turn.

Figure 12. Focusing due to sonic cutoff and in-plane steady turn.

utilized: hypersonic finite-difference calculations for the near-field flow, wind-tunnel measurements to obtain purely empirical F-functions, and theoretical analyses based on tractable simplified conditions.

Wind-tunnel measurements of launch and reentry vehicles (refs. 47 and 48) have clearly demonstrated the ability to measure F-functions at hypersonic speeds and for blunt bodies. Subsequent use of these F-functions as inputs to boom calculations has been very successful. An associated task of this type of study was the calculation of selected points via a finite-difference computer code. In references 48 and 49, a 1970's vintage code was utilized, with very good agreement with wind-tunnel data.

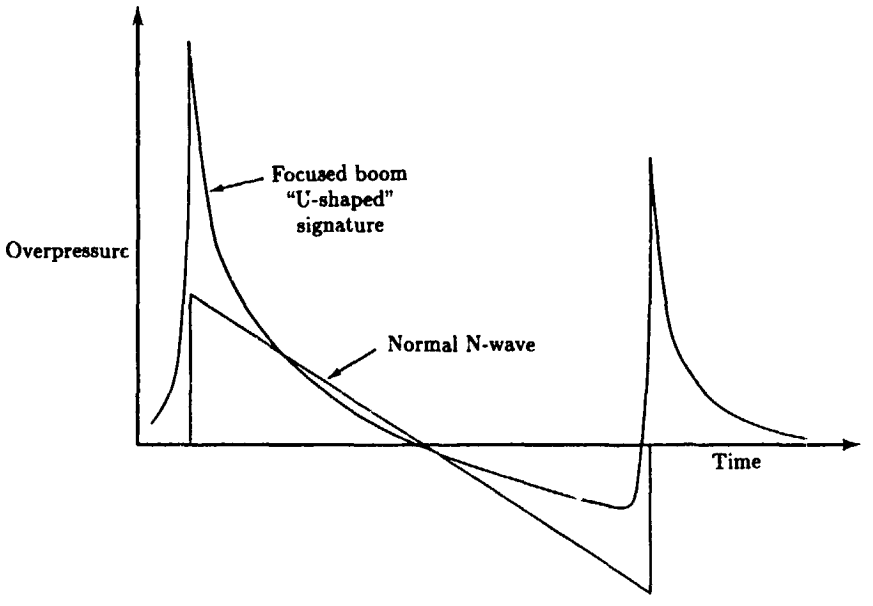

Figure 13. Focused and unfocused boom signatures.

With continued improvements in computational fluid dynamics and ever-lowering computer costs, it should be practical to use Euler codes to compute complete F-functions for hypersonic speeds. No such application has yet been made, but it is an expected development for current hypersonic projects.

One theory for hypersonic booms is available, that developed in reference 50. It is based on a concept by Seebass (ref. 51) that even slender hypersonic vehicles effectively have blunt noses (both physically, because of heating considerations, and aerodynamically, because of the entropy layer), and the resultant drag dominates the sonic boom. The model of such a vehicle is a spherical nose on a very slender, infinite afterbody, very much like the physical model used for the hypersonic-boom wind-tunnel study of reference 49. The far-field wave pattern of such a body can be computed by means of a blast wave analogy. Reference 50 contains a careful analysis of this configuration, identifying the significant terms in the hypersonic flow equations, writing the appropriate similitude-scaling laws, and matching near-field flow (where entropy layer effects are important) with the far field (where entropy layer effects can be argued to be negligible). Quantitative results for the far field were presented, with constants incorporated from a numerical solution to the equivalent blast wave. The analogy is valid for the positive-pressure phase of the far-field N-wave Δp (the positive impulse I) and also provides an estimate of the location of the trailing shock. The final far-field sonic boom results were combined with geometrical acoustics atmospheric corrections for an isothermal model atmosphere. Figure 14 shows the final prediction; this figure is based on reference 52, which contains a synopsis of reference 50. The only vehicle parameter is drag, as might be expected from the nature of the theory. In reference 50, agreement with reentry data for the blunt-body spacecraft is reasonably good.

The reference 50 theory predicts hypersonic transport (HST) sonic boom levels which are apparently lower than those established for supersonic transports. Shown for comparison in figure 14 are Δp and I for a nominal 400 000-lb SST at $M = 2.7$. The SST boom is significantly greater than the HST boom. This type of comparison has led to speculation that hypersonic transports may have a sonic boom advantage. However, there are two points to consider. First, the theory is effectively a volume-only model and does not account for vehicle lift. Almost 40 percent of the example SST boom is due to lift. An extension of the theory to account for lift-induced boom, analogous to Walkden's theory at supersonic speeds, would be very useful but has not yet been attempted. Second, the drag-dominated theory implicitly assumes a short body. This assumption results in durations considerably shorter than those calculated for the SST, with a correspondingly lower impulse.

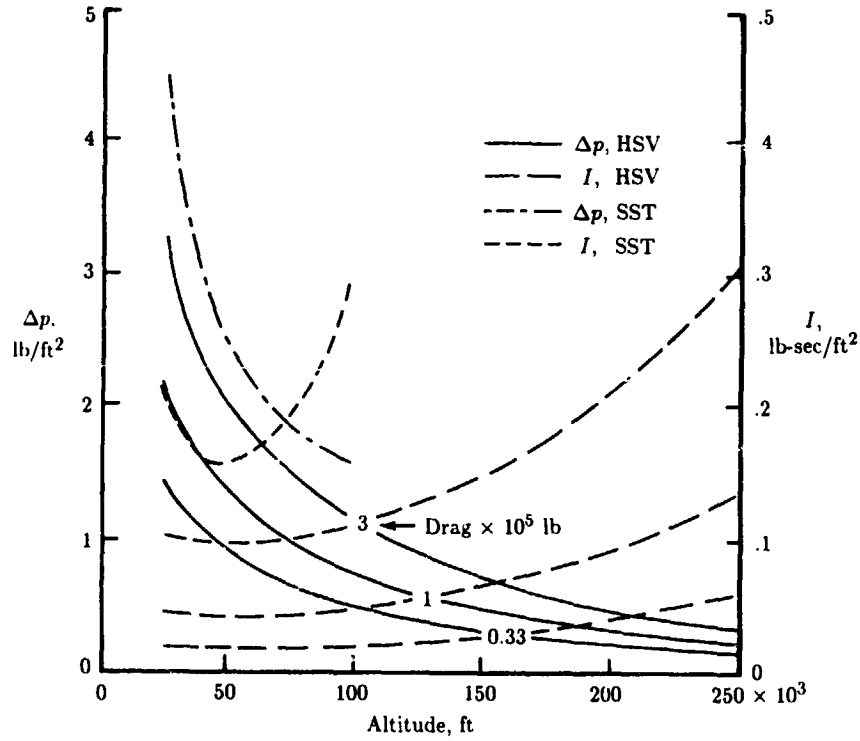

Figure 14. Overpressure and impulse as function of altitude for drag-dominated hypersonic vehicle. Conventional SST shown for comparison. (Based on ref. 52.)

Measurements and Predictions

This section deals with the primary boom carpets for both steady, level flights and for aircraft in maneuvers. For steady, level flight, both on-track and lateral measurements and comparisons with predictions are presented. Variability in the sonic boom measurements as a result of the atmosphere is presented and changes in waveform and probability distributions of measured-to-predicted boom levels are

shown. Focus booms associated with various types of operations, their ground patterns, and the pressure buildups are described. Finally, recent experience with secondary boom carpets is discussed, including the signature characteristics and amplitudes of the booms.

Primary Boom Carpets for Steady, Level Flight

On-Track Measurements

A considerable number of studies have been conducted which were aimed at defining the peak amplitudes (overpressures) of the signatures for primary boom carpets for a wide range of vehicles and flight conditions. A summary of these results is shown in figure 15. Predicted and measured on-track sonic boom overpressures are plotted as a function of altitude for several aircraft of various sizes and weights (including Concorde) along with measured data for the launch and reentry phases of the Apollo 15, 16, and 17 spacecraft (ref. 53), and the Space Shuttle ascent and reentry flights (ref. 54). Measured and predicted values of overpressure correlate well for the aircraft cases. The sonic boom levels in general increase with increasing aircraft size and decrease with increasing altitude. The theory is valid for direct booms of conventional aircraft.

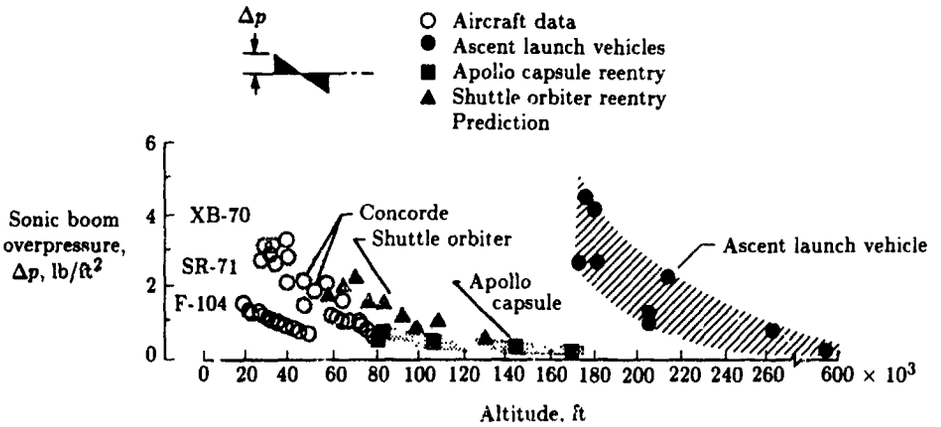

Figure 15. Measured and predicted on-track sonic boom overpressures in primary carpet area for several aircraft and spacecraft.

For measurements made during the reentry of spacecraft, the measured data are consistent with data obtained for aircraft in that they appear to be comparable in magnitude to extrapolated levels for fighter or medium bomber aircraft and they display a similar decrease with increased altitude.

In general, the measured overpressures for the launch and ascent portion of spacecraft flights indicate the same trend of decreasing pressure with increasing altitude. However, the magnitudes of the overpressure values are much greater than those of the reentry case. Since the launch vehicle is considerably larger than the reentry vehicle, higher boom levels can be expected. However, the largest portion

of the increased overpressure from launch vehicles results from the "effective body" produced by the rocket exhaust plume. Note that disturbances from the ascent phase, with engines thrusting, were measured at ground level for the vehicle operating at altitudes up to about 600 000 ft (ref. 55). Simplified methods for prediction of spacecraft sonic booms are discussed in references 36 and 48.

Lateral Spread Measurements

Considerable attention has also been given to defining the lateral extent of the primary boom carpet for steady flights of aircraft at various Mach numbers and altitudes. The calculated and measured primary carpet data for 13 flights of the XB-70 at $M \approx 2.0$ and an altitude of 60 000 ft are shown in figure 16. These data are also typical of other aircraft and operating conditions. At the top of the figure an approaching supersonic aircraft is schematically shown, along with the downward-propagating rays. The extent of the primary carpet is the point at which the ray refracts away from the ground (the cutoff distance). This lateral cutoff point is independent of aircraft type and is only a function of the aircraft altitude, the Mach number, and the characteristics of the atmosphere below the aircraft.

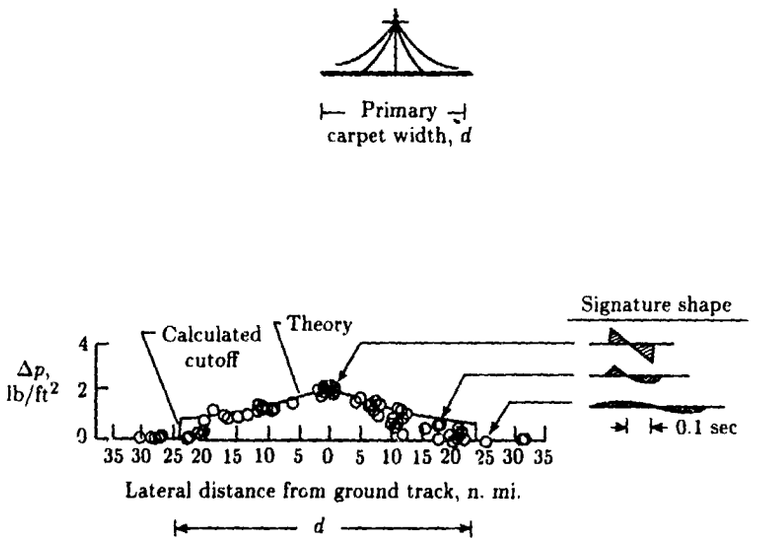

Figure 16. Sonic boom overpressures for XB-70 aircraft at an altitude of 60 000 ft as function of lateral distance. $M \approx 2.0$.

Comparisons of the calculated and measured lateral extent of the sonic boom patterns as a function of aircraft altitude and Mach number for steady flight in a standard atmosphere are given in figure 17. The data points represent averages of a number of measurements involving various aircraft. The widths of the sonic boom carpets on the ground increase with increasing altitude and Mach number. For example, at an altitude of 20 000 ft and $M = 1.5$, the total width of the pattern is 20 n.mi. At 60 000 ft and $M = 2.0$, the pattern width is about 60 n.mi. However, as is illustrated by the two sketches at the top of the figure, supersonic flights at low altitudes result in narrow carpets having higher overpressures, whereas at higher

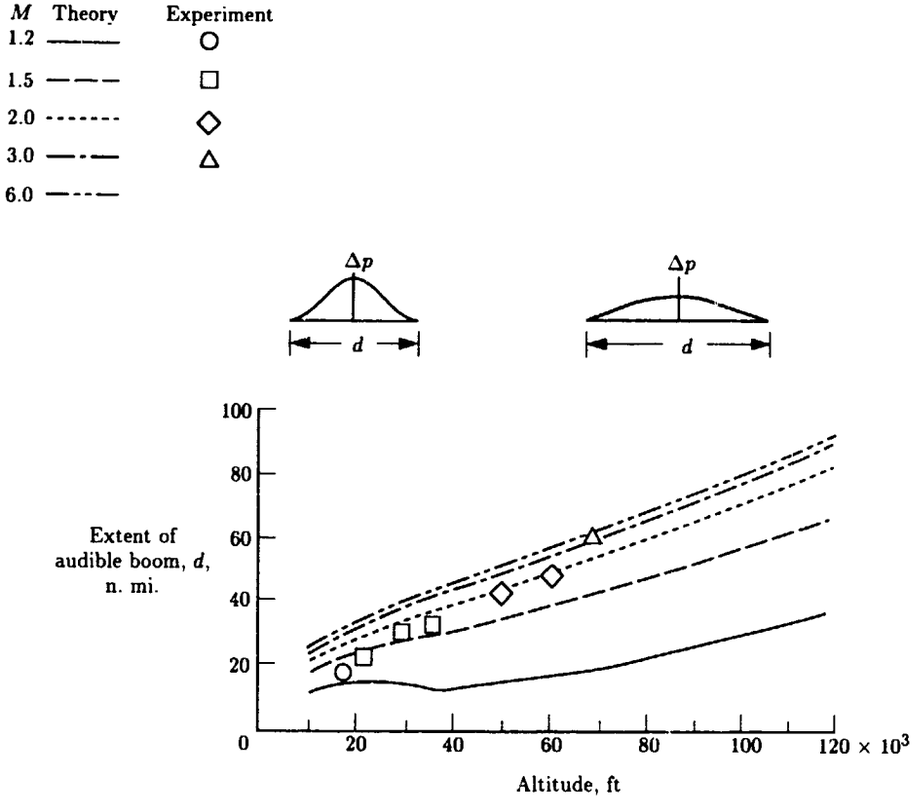

Figure 17. Width of area of audible sonic boom pattern on ground.

altitudes the carpet widths are much broader but with lower ground overpressures. Good agreement exists between measured and calculated values. The hypersonic aircraft will operate at altitudes and Mach numbers beyond the current experience. However, there is no reason to believe that theory would not provide reasonable estimates of the carpet width for this anticipated flight regime.

Variability Due to Atmosphere

The boom signatures associated with the on-track and lateral measurements were measured under fairly stable atmospheric conditions. It has been noted previously that atmospheric variations, particularly those in the first few thousand feet above the Earth surface, can be very influential in bringing about distortions of the sonic boom signature (see fig. 5), changing it from the normally expected N-wave to a "peaked" or "rounded-type" signature (ref. 56). Higher overpressures result when the signatures are peaked, whereas lower pressures are associated with rounded signatures. This peaking and rounding of the boom signatures is statistical in nature and occurs as a function of either time or distance.

A summary of the variations of the on-track overpressures resulting from the atmosphere for steady, level flight is given in figure 18. This statistical analysis comprises most of the planned sonic boom experiments that have been conducted in

the United States. Data are included for a wide range of aircraft, a Mach number range of 1.2 to 3.0, and an altitude range of about 10 000 to 80 000 ft. A total of 12 406 data samples have resulted from 1625 supersonic flights.

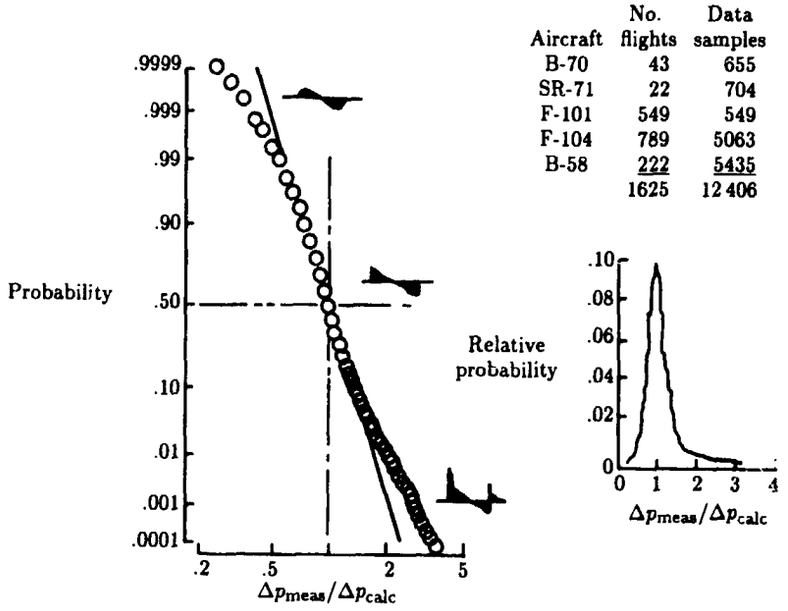

Figure 18. Statistical variation of sonic boom waveforms and overpressures resulting from atmosphere for steady, level supersonic flight.

Plotted on figure 18 is a relative cumulative frequency distribution and histogram for on-track measurements showing the probability of equaling or exceeding the ratio of the measured overpressure to the calculated or nominal overpressure for steady flight in standard atmosphere. For this type of presentation, all the data would fall in a straight line if the logarithm of the data fit a normal distribution. Rounded signatures of the waveform sketched in the figure are usually associated with overpressure ratios less than 1. Nominal or N-wave signatures are observed on the average, and peaked signatures of higher overpressures are observed usually at ratios greater than 1. The data of figure 18 indicate that variation in the sonic boom signatures as a result of the effects of the atmosphere can be expected during routine operations.

Primary Boom Carpets for Maneuvers

Any rapid deviation of a vehicle from steady, level flight conditions can produce considerable modifications in the location, number, and intensity of the ground shock wave patterns. This maneuvering phenomenon is illustrated in figure 19, which shows the shock wave ground-intersection patterns for two flight conditions of an aircraft (ref. 57). For simplicity, only the bow shock wave is shown.

At the left in figure 19 the lateral spread pattern on the ground for an aircraft in steady, level flight is shown. The ray paths on the ground, represented by the angled

lines, are generally parallel to each other, and the shock wave ground-intersection patterns, as represented by the heavy lines, are essentially hyperbolic in shape. The pattern to the right is for an aircraft experiencing a lateral acceleration. The ray paths are no longer parallel; in fact, in some regions they tend to converge and in others to diverge. Likewise, the shock wave ground-intersection pattern is no longer hyperbolic and contains some irregularities, including a shock fold in which multiple booms would be observed and a cusp formation in which the pressures are higher than for steady flight conditions. Such pressure buildups correspond to focused superbooms discussed previously.

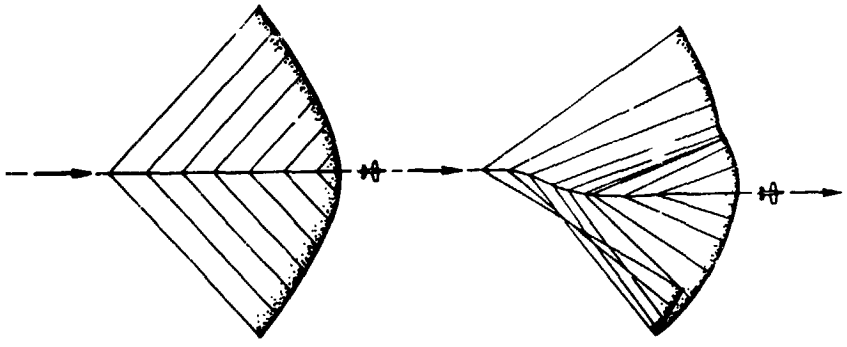

Figure 19. Shock wave ground-intersection patterns for aircraft in steady and accelerated flight at constant altitude. (From ref. 57.)

Sonic boom enhancement can result from a variety of aircraft maneuvers. Figure 20 illustrates three types of maneuvers which could result in pressure buildups at ground level: a longitudinal acceleration, a 90° turn, and a pushover maneuver. In each maneuver, pressure buildups occur in the localized regions suggested by the shaded areas in the sketches. It is very important to remember that although the aircraft and shock waves are moving, these localized areas on the ground in which pressure buildups occur are fixed and do not move with the aircraft. The localized regions, incidentally, are on the order of 1000 ft or less in width. The pressure buildups in these focus areas are a function of the type of maneuver and the acceleration involved and are noted in the *Review and Status of Theory* section to be 2 to 5 times the boom carpet values. As noted previously, pressure buildups will always result for the longitudinal maneuver when the aircraft accelerates from subsonic to supersonic speeds. The pressure buildup areas associated with turns and pushover maneuvers can be minimized or avoided by reducing acceleration (or decelerating) or by simply avoiding the maneuver.

In scheduled commercial operations, longitudinal acceleration from subsonic to supersonic speeds is the only maneuver of significance from a ground exposure point of view. Experience has demonstrated that the focus boom region associated with this acceleration can be placed to within about 2 miles of the designated area.

It is important to note that any randomness of the atmosphere, which brings about waveform distortions discussed in connection with figure 18, may decrease the focus factor value and, for certain situations, may eliminate the focus altogether.

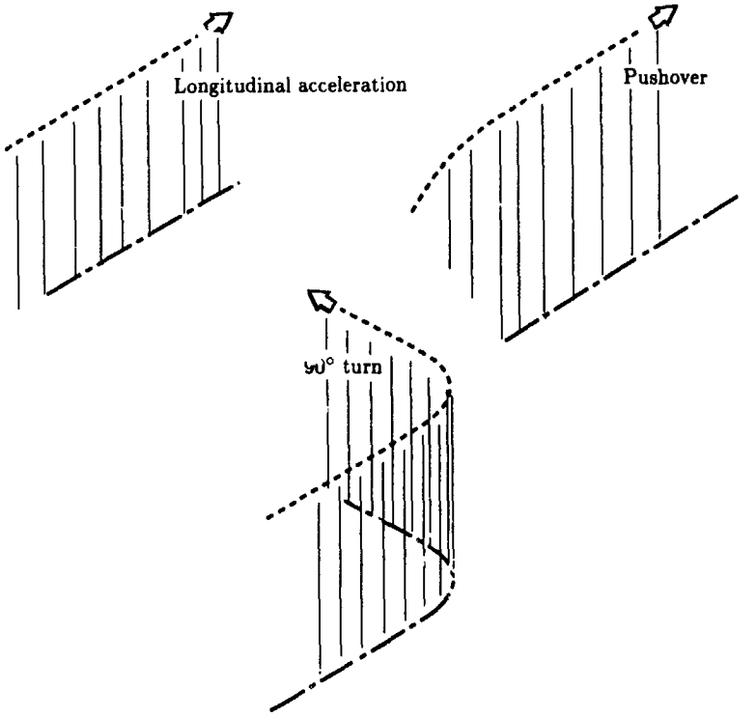

Figure 20. Areas on ground exposed to superbooms resulting from three maneuvers.

Secondary Boom Carpets

Secondary sonic booms, or so-called "over-the-top" boom disturbances (refs. 10 to 15), are quite distinct from primary booms, not only in the manner in which they are propagated from the aircraft to the ground but also in the way their signatures are shaped. The characteristics of these secondary sonic booms are illustrated in figure 21. An overall pressure time history (ref. 15) from the Concorde for a secondary boom is shown in figure 21(a). Note the signal is complex in that a number of disturbances are observed at this particular measurement location over a period of 1.5 minutes with a maximum peak-to-peak pressure of about 0.2 psf. Three sections of the overall pressure signature at A, B, and C are presented with expanded time scales in figures 21(b) to 21(d) to provide an indication of the frequency of these signals. Note that the fundamental frequency is about 1.5 to 2.0 Hz. For secondary boom signatures, the pressure changes very slowly and is in the subaudible frequency range. This, combined with the very low amplitudes, makes it difficult for the ear to sense this sound. These secondary booms are heard, however, and descriptions vary from the rumbling of far-off thunder to startling. Indoors, of course, such a pressure signature can be more noticeable since it vibrates the structure and causes rattling and motions.

Secondary booms have existed since the beginning of supersonic flight capabilities. Each of the major sonic boom flight programs sent secondary booms propagating through the upper atmosphere. These secondary booms went essentially unnoticed

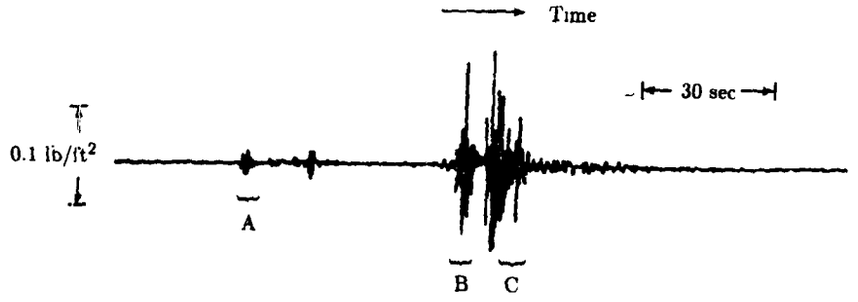

(a) Overall pressure time history.

(b) Expanded pressure time history at A.

(c) Expanded pressure time history at B.

(d) Expanded pressure time history at C.

Figure 21. Characteristics of secondary sonic booms.

until the 1977 to 1978 time period, when the Naval Research Laboratory investigated the east coast acoustic disturbances (ref. 58), which were initially reported to be strange and mysterious in origin. The Concorde had entered into commercial service in mid-1976, of course, and scientific use was being made of its secondary boom, which was a consistent and known source, for determining the characteristics of the upper atmosphere (refs. 12 and 13). Concorde secondary booms thus became more evident and complaints to this effect were received. However, in every case of Concorde-generated secondary sonic booms, rerouting of the flight tracks and changes in operating conditions, depending upon atmospheric and seasonal variations, eliminated the problem.

The secondary sonic boom carpet and the disturbances experienced within it are not as well defined as for the primary sonic boom, and only fragmentary observations and measurements are available. These disturbances are known to involve both the upper and lower levels of the atmosphere during propagation, to have very low overpressure values, and to have a very low frequency content. Propagation distances greater than 100 miles are common and relatively large ground areas are exposed, but the significance from a community response standpoint is not well-defined.

Sonic Boom Minimization

This section addresses sonic boom minimization through aircraft design and aircraft operation. Minimization through design involves modification of the aircraft size, weight, and shape in order to reduce the overpressure or to alter the waveform. Minimization through aircraft operation relates to flying the aircraft at a Mach number and altitude combination so that a boom does not reach the ground. The atmosphere plays a significant role in this process. Mention is made of sonic booms from aircraft at transonic Mach numbers ($0.89 \leq M \leq 1.00$) and relatively low altitudes, and the associated waveform and boom levels are discussed.

Design

Sonic boom effects are minimized through increased distance between the aircraft and the ground. Minimizing sonic booms through aircraft design modifications has also been investigated and lower bounds have been established (refs. 52 and 59 to 62). Some of the approaches that have been considered are illustrated in figure 22. Sonic boom minimization can be achieved through a reduction in the overpressure or an increase in the signature rise time, each of these parameters being significant with regard to human response (refs. 63 and 64) and to structural response (ref. 65). Altering the overpressure and the rise time also results in changes in impulse. As illustrated in the lower sketches of the figure, reduced overpressures can be obtained by reducing the size of the aircraft (that is, lower aircraft weight and volume) or by proper shaping of the aircraft geometry to provide a modified (i.e., flattop) signature. The minimum impulse signature is generally that of an N-wave. The minimum overpressure is that of the flattop and flat-bottom N-wave. These two approaches have been given consideration in the past, and reductions in bow wave overpressures of about 30 percent to perhaps as much as 40 percent appear to be obtainable.

Other minimization techniques involving increasing rise times have also been investigated (refs. 66 and 67). If the rise time of the signature could be increased to

the point where a sine wave would result instead of an N-wave, the sine wave pressure signature should not be audible to an outdoor observer. However, this avoidance of the shock wave altogether would result in an increased impulse, and such a signature would still vibrate buildings such that people indoors would react. To obtain even small increases in rise times, the aircraft length would have to be increased by at least a factor of 3 over the greatest length now being considered (to about 1000 ft). This in itself is an impractical approach. Another means would be to alter the airstream so that the same beneficial effects associated with the increased length are obtained. This would be accomplished by the addition of heat or other forms of energy. Studies of the airstream alteration or the "phantom body" concept suggest that large amounts of heat or energy (at least the equivalent of the output from the onboard propulsion systems) are required to obtain increased-rise-time signatures. This approach therefore also appears to be impractical.

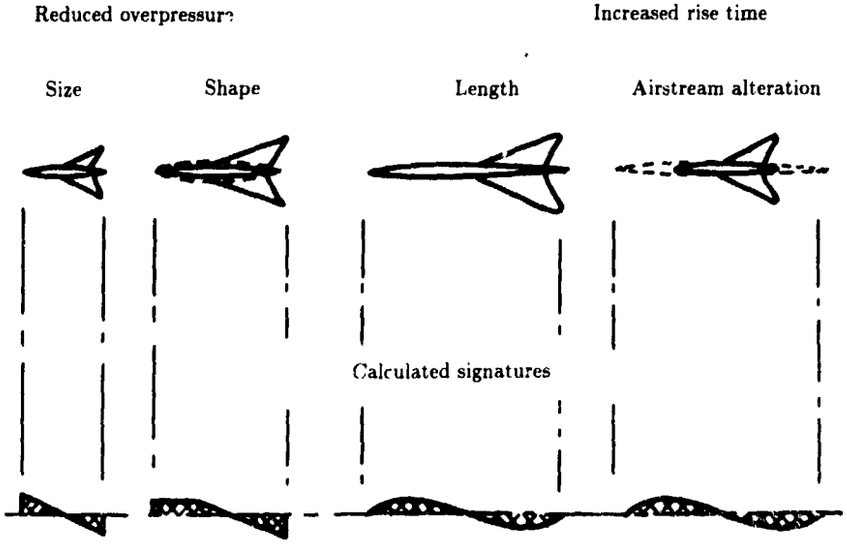

Figure 22. Sonic boom minimization concepts.

As a result of past and current efforts in boom minimization, it is generally agreed that the nominal cruise sonic boom signatures can be modified through aircraft design. Absolute lower bounds are available for overpressure and impulse. The significant advances which have been made in propulsion, materials, and aerodynamics will play a significant role in reducing sonic boom levels. For example, supersonic laminar flow exerts a very powerful influence on reducing aircraft gross weight and increasing cruise altitude, both of which lower the sonic boom level. In-house NASA studies (ref. 68) suggest the feasibility of a long and light SST having a sonic boom overpressure level of less than 1.0 lb/ft^2 (about half the overpressure estimated for the canceled U.S. SST) during cruise flight for domestic ranges. The analytic tools for defining the required aircraft characteristics are available and have been validated with wind-tunnel experiments on small wing-body configurations representing transport aircraft. Means for evaluating the trade-offs for boom minimization in terms of actual aircraft design are available. The most

desirable signature shape, from the point of view of minimum response of an outdoor and indoor observer and of structural response, has not yet been established.

"Boomless" Flight Operations

In addition to sonic boom minimization, sonic boom avoidance can also be realized through operation of the aircraft at low supersonic Mach numbers such that the shock waves extend down toward, but do not intersect, the ground because of atmospheric refraction or cutoff, as suggested by the sketch in the upper left of figure 23. The range of Mach numbers and altitudes over which operations at cutoff Mach number M_{co} can be performed is shown in the figure for steady, level flight in a standard atmosphere with no wind. Flights at Mach numbers to the left of the hatched curve will result in no booms reaching the ground, whereas flights at Mach numbers to the right of the curve will result in booms reaching the ground. The highest speed at which the aircraft could operate in a standard atmosphere without producing booms at the ground is about $M = 1.15$. In the real atmosphere, variations in the speed of sound do exist because of temperature and winds. Climb or descent angles would also permit an increase or decrease in M_{co}, respectively. The practical range of M_{co} varies from 1.0 to about 1.3 for steady, level flight for a fairly wide range of atmospheric conditions.

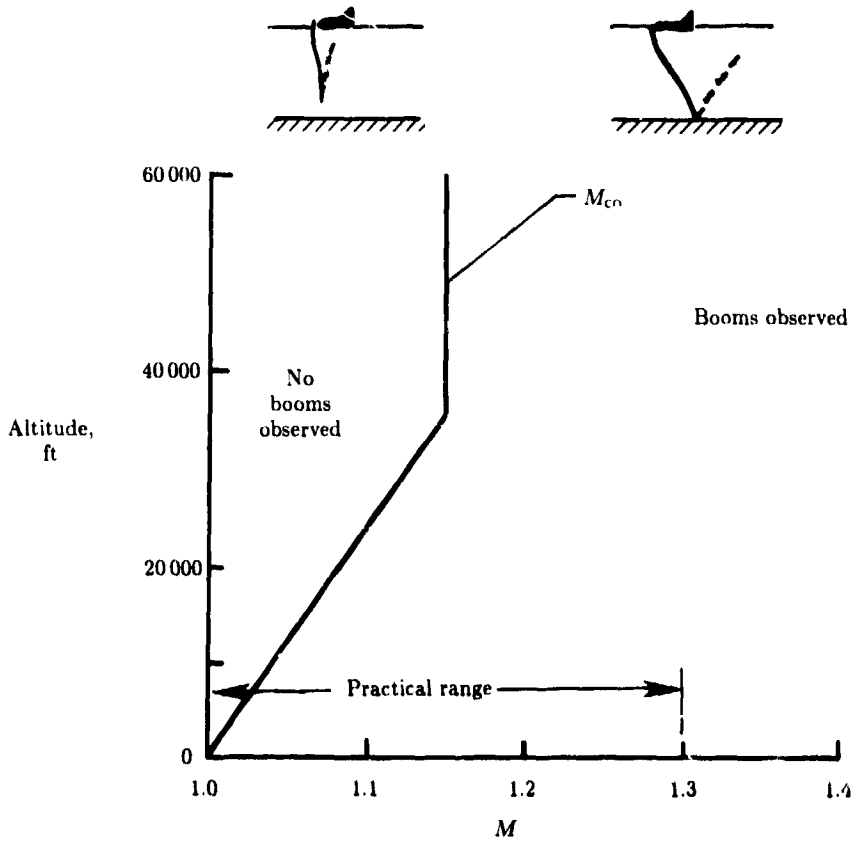

Figure 23. Combinations of Mach number and altitude for boomless flight.

Two points should be made about boomless flight operations. Boomless flight is independent of aircraft configuration and is a function of the aircraft operating conditions and the atmosphere. Aircraft configuration is, of course, important from the standpoint of efficiency of operation at these low Mach numbers; for example, flying a high Mach cruise design at the off-design M_{co} is less desirable than flying an aircraft designed to operate at $M = 1.15$. In either case, boomless flight operations, unlike the stationary focus from an aircraft maneuver, always result in a continuous caustic or focal line where the overpressures can be higher than those of the steady-flight boom from the aircraft flying at the same altitude but at the higher cruise Mach number. Therefore, in order to assure the shocks, and thus the boom, for flight at M_{co} will terminate at some safe height above ground level, a margin of safety in the form of reduced Mach number is required.

Low-Altitude Transonic Flight

It can generally be stated that as long as the aircraft speed over the ground is less than the speed of sound at the ground, then boomless flights at low supersonic Mach numbers can be achieved. It may be further stated that as long as the aircraft speed is less than $M \approx 1.00$, no sonic booms should be experienced at ground level. This is true for aircraft flying at altitudes of 100 body lengths or greater. Experience, confirmed by measurements (ref. 42), indicates that booms can be observed at ground level from aircraft in steady, level flight at Mach numbers from about 0.95 to 0.99 at altitudes of about 300 to about 2000 ft above ground level. This phenomenon is similar to that observed for airfoils in wind tunnels (as shown in fig. 24(a)) at high transonic Mach numbers, for which localized shocks occur at the maximum thickness (where the flow accelerates to $M = 1.00$ or greater). These shocks extend for some distance from the airfoil before dissipating into acoustic disturbances. This extended shock is also shown in the unusual photograph of an aircraft in flight at an indicated Mach number of 0.89 and an altitude of about 300 ft (fig. 24(b) from ref. 69). The explanation for why the shock waves are visible is given in reference 69 as follows. "Aircraft is flying in a cloud of water vapor condensed by a shock wave created when the local Mach number reaches or exceeds 1.0 at a point on the fuselage aft of the cockpit, where the shock attaches." The basic mechanism involved in the flight picture is the lower pressure behind the shock front causing the moisture in the air to condense.

The aircraft, like the airfoil, has a maximum thickness (equivalent area distribution) such that the local flow can equal or exceed $M = 1.0$ at some given free-stream transonic Mach number. These localized shocks have been observed to extend outward and downward as much as 30 airplane body lengths. The intensity of the booms is substantial because of the very low altitudes, and the signature, shown in figure 25, is considerably different in nature from the normally observed N-wave-type signature associated with a fully developed supersonic flow field.

The detailed analysis of low-altitude transonic flight test data (ref. 42) has indicated that existing meteorological conditions influence the vertical extent of attached shock waves produced at nearly sonic flight. Aircraft Mach number also has a direct influence on the vertical extent of the attached shock waves. The extension of these attached shock waves to lower altitudes may explain several "accidental" sonic booms produced by low-altitude, marginally subsonic aircraft (although Machmeter and altimeter errors may also be responsible).

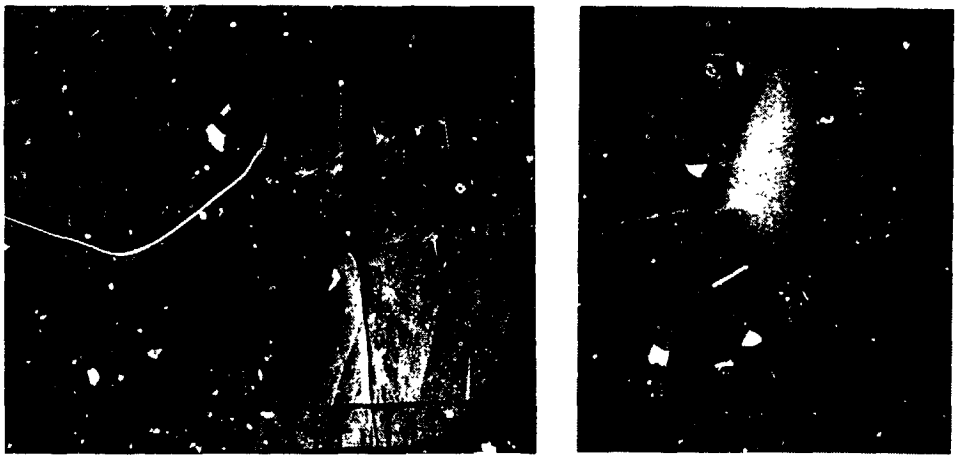

(a) NACA 16-212 airfoil in wind tunnel. M = 0.90.

(b) Aircraft in transonic flight. M = 0.89. (From ref. 69. Copyright Paul A. Ludwig.)

Figure 24. Transonic flow fields.

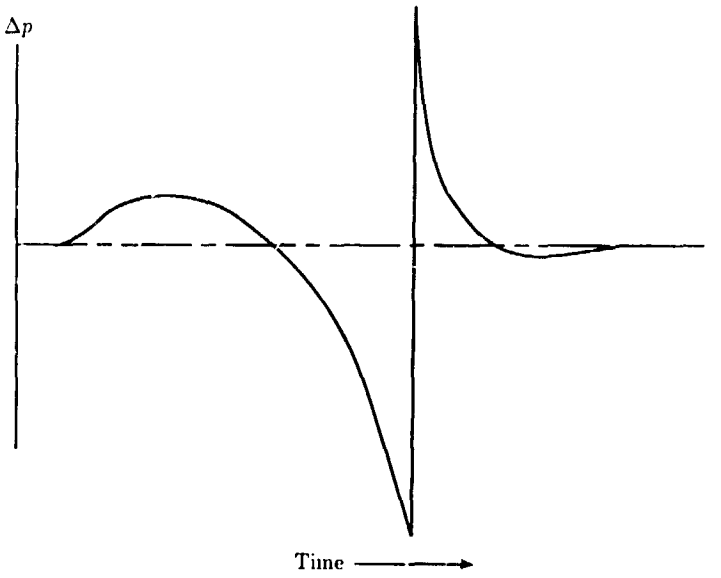

Figure 25. Character of transonic boom signature.

Responses to Sonic Booms

This section begins with a description of the factors involved in boom exposure, including the air path, ground path, and building vibration. Outdoor and indoor stimuli include audible, vibratory, and visual cues. A discussion of damage complaints, relative to primary and secondary structural members, is given as a function of the range of boom exposure levels. People responses to booms include startle,

annoyance, effects on sleep, and long-term effects on health. Other responses to sonic booms cover animals, birds, and fish, and also include seismic effects, avalanches, landslides, and other subsonic aircraft.

Factors Involved in Boom Exposures

There is considerable concern about the manner in which people and structures respond to sonic booms and how such responses will affect community acceptance of overland operations. The nature of the response problem is illustrated in figure 26 (from ref. 70). The sketch at the top of the figure suggests two different exposure situations for people. In one case, the person is outdoors and is impinged on directly by the waves. In the other case, the observer is inside a building and the waves impinge first on the building. The building then acts as a filter which determines the nature of the exposure stimuli reaching the inside observer. The ingredients of this indoor exposure situation are included in the chain diagram at the bottom of the figure. The sonic-boom-induced excitation which causes the building to vibrate may arrive either through the air or through the ground. It is generally conceded that the air path is the more significant one in most cases and is thus designated the primary path in figure 26. The ground path is considered secondary and is designated by a dashed line in figure 26. Building vibrations can be observed directly by the subject. A person may also observe vibration-induced noise or, in the extreme case, associated superficial damage of the structure.

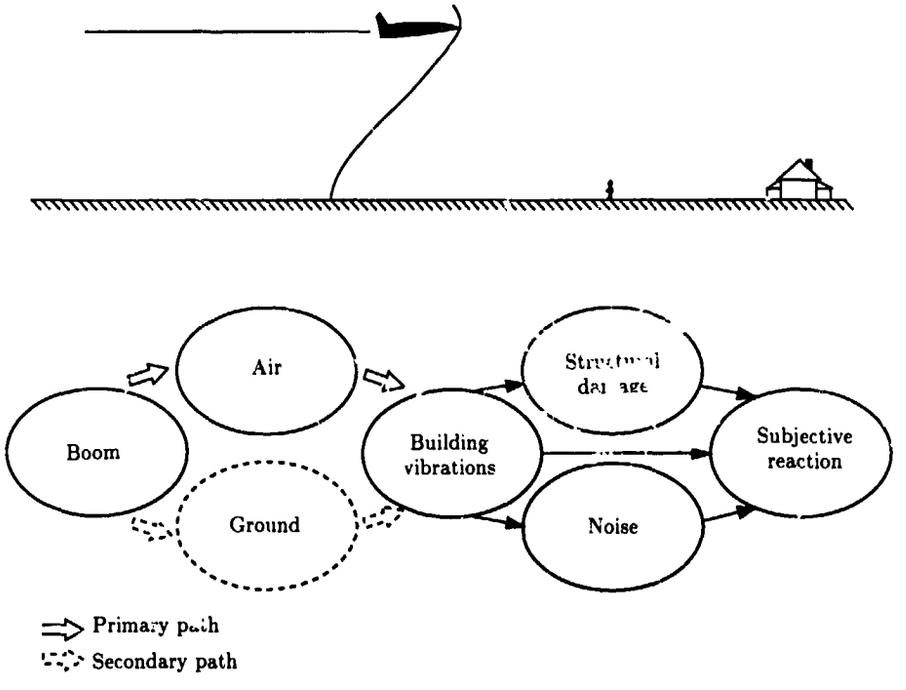

Figure 26. Factors involved in boom exposures. (From ref. 70.)

Outdoor and Indoor Stimuli

A person inside a building is exposed to a rather complex series of stimuli, including auditory, visual, and vibratory inputs. The nature of the auditory and vibratory inputs is illustrated in figure 27 (from ref. 70). The top trace is a sample outdoor pressure exposure as measured for one particular case. This wave is of the N-wave type, but it differs from an N-wave in some of its details, as do many of the waves measured in the field. The three bottom traces represent corresponding indoor exposure stimuli. The topmost of these traces represents the pressure variation inside the building owing to vibratory motions of the building and the cavity resonances. Although this is a pressure disturbance, it generally occurs in a frequency range that is not audible to humans. The audible portion of this signal, as measured with a separate microphone system, has the characteristic shape of the middle trace and is an order of magnitude lower in amplitude. It is believed that this audible portion of the pressure signal is associated with the rattling of the building structure and furnishings because of the primary mode responses in the building. Finally, the bottom trace represents the vibration of the floor that would be sensed by a person either directly or through the furniture. A person indoors therefore can be influenced because of an auditory, vibratory, or visual cue. At the present time, the indoor exposure situation is not understood well enough to permit the relative importance of each of these stimuli to be determined, although it is believed that in certain situations each one is significant.

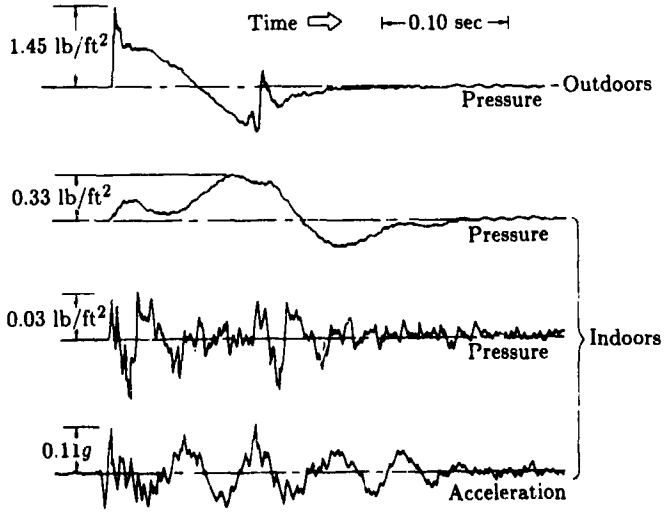

Figure 27. Outdoor and indoor sonic boom stimuli. (From ref. 70.)

Damage Complaints and Range of Boom Exposures

Experience has shown that supersonic flights over communities have resulted in complaints regarding damage because of sonic booms. The nature of the reported damage is fairly well represented by the data in figure 28, which shows the frequencies

with which certain types of damage are mentioned (ref. 6). Plaster cracks, the type of damage reported most frequently, are mentioned in 43 percent of the complaints. Other reported damage includes cracks in window glass, walls, and tile. Structures reportedly damaged by sonic booms are mostly brittle surfaces and are secondary structural components.

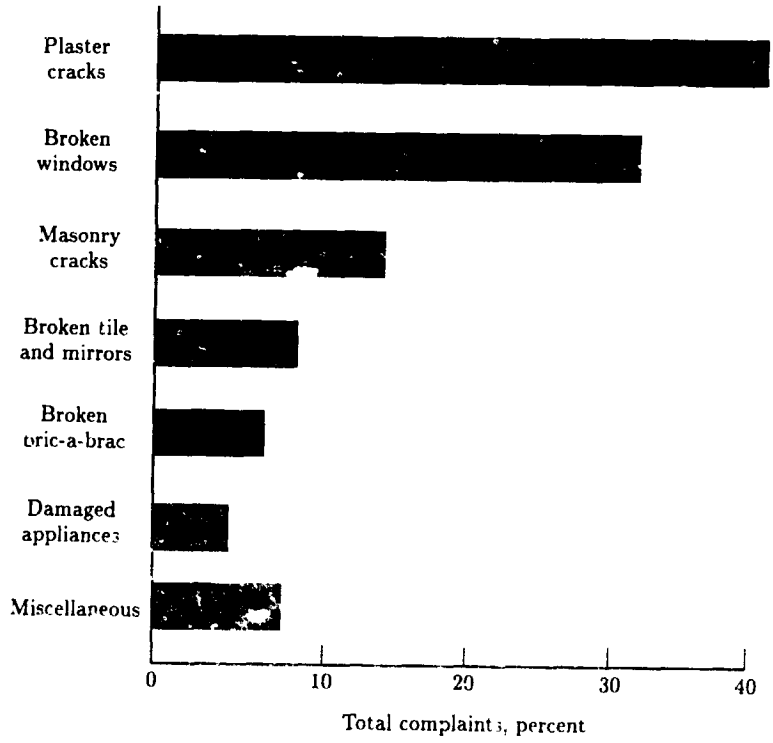

Figure 28. Sonic boom damage complaints. (From ref. 6.)

The relation between sonic booms and damage has the same complexity as the relation between sonic booms and indoor responses: a rigorous relationship depends on the frequency content of the boom and the frequency response of the structure. A practical, simple measure of the boom (for correlation with damage) would be the energy content in frequencies around the fundamental response frequency of structures, since this is where the greatest response occurs (refs. 65 and 71). Previously in this chapter the argument was presented that aural response to sonic booms can be quantified by the peak overpressure, since that was associated through audio frequency components of booms. Similarly, it can be argued that structural response involves low frequencies, so that the impulse of the boom is an appropriate quantity. For this reason, boom impulses, as well as peak overpressures, are often reported. The boom impulse tends to represent the lowest frequency components, in the range of several hertz. The fundamental frequency response of buildings is typically 10 to 30 Hz (ref. 72), however, so impulse alone may not be an adequate measure.

The vast majority of experience with sonic booms has been with N-waves 200 to 300 msec in duration. Usually only the overpressure has been reported or correlated with damage. One would, however, expect the relation between impulse, spectra, and overpressure to be fairly consistent for booms of such similar shapes. Care must be taken when these data are applied to significantly different types of boom signatures, but these correlations of boom damage with overpressure should certainly be self-consistent and well worth examining.

As expected, the reported damage varies depending upon the intensity of the boom. This is illustrated in figure 29, in which sonic-boom-induced incidents per flight per million people are shown for various overpressure ranges (ref. 6). The ranges of boom levels up to about 3.0 lb/ft^2 are fairly representative of the majority of booms associated with controlled supersonic flight operations. It may be significant that no damage incidents occurred for boom exposures below about 0.8 lb/ft^2, although a smaller number of data samples were available in this range.

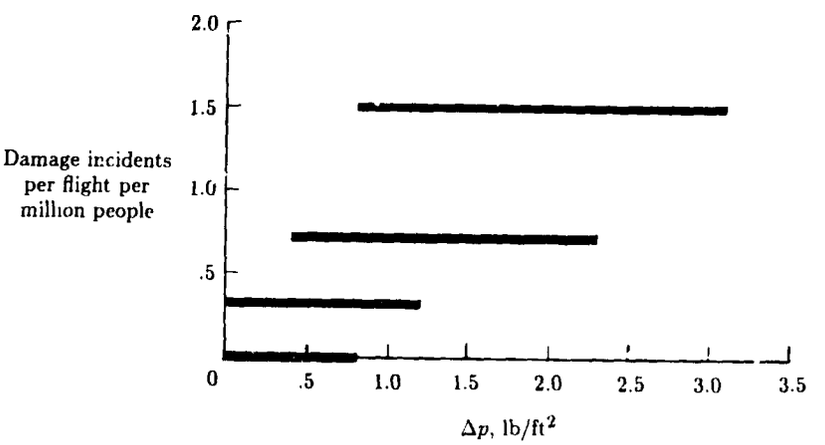

Figure 29. Sonic-boom-induced incidents for various overpressure ranges.

The nature of the sonic-boom-induced damage problem can be illustrated with the summary plot of figure 30 (from ref. 6). The number of damage incidents for a given type of structure increases as the overpressure increases, and this is particularly evident at the higher overpressure values. Also shown in the figure is a schematic illustration of the amplitude distribution of the overpressures. Even though the nominal, or predicted, overpressure for a given aircraft at specific flight conditions has a value which is generally lower than that at which building damage might be expected, there is a distribution of pressure amplitudes such that a small percentage of the total amplitude values occurs in the relatively high overpressure range. These high values, which occur only occasionally because of either atmospheric effects or focus booms due to maneuvers, may be sufficient to trigger incipient damage in existing structures. Two points can be made from this figure. It is obvious that a lower nominal value is desirable because of the reduced probability of building damage. However, though the nominal overpressure is established at a relatively low value, no assurance can be given that the triggering of damage can be completely avoided.

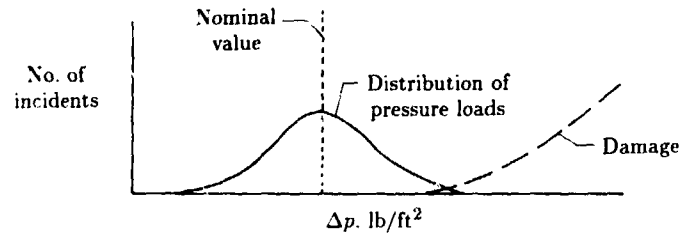

Figure 30. Nature of sonic-boom-induced damage problem. (From ref. 6.)

People Responses

It has been shown that people are annoyed by sonic booms because of concerns that the booms may damage their property. This suggests that the annoyance of booms might be diminished if the public could be convinced that boom levels from military or commercial supersonic operations are well below the damage threshold. However, sonic boom effects on people are difficult to pinpoint because of the subjectivity of the people's responses and because of the diversity of variables affecting their behavior. Responses depend on previous exposure, age, geographic location, time of day, socioeconomic status, and many other variables.

Research and experimentation have turned to several findings about sonic boom phenomena related to humans. These findings indicate that booms do not adversely affect human hearing, vision, or circulation (ref. 6). The human psychological response is more complex, involving attitudes and habituation to booms and their sources.

There findings have also turned up a number of other points. Long-term effects on health of repeated daily booms have not been investigated. Possible long-term effects on sleep of repeated night booms are unknown. Although existing evidence suggests booms of 1.0 lb/ft^2 or greater are unacceptable to a significant portion of the population, a level of acceptability of sonic booms has not been determined. Values of sonic boom overpressure of 0.5 to 1.0 lb/ft^2 have been suggested, but with no scientific support.

Finally, the possibility exists that human responses to booms measured one to two decades ago may differ from those recorded in the next decade (ref. 6).

Other Responses

To date, it has been difficult to make detailed interpretations of the effects of sonic booms on different animal species. However, research on chickens, chicken and pheasant eggs, pregnant cows, racehorses, sheep, wild birds, and mink suggests that boom effects on domestic and wild animals are negligible (ref. 6). Like humans, animals are startled by loud noises, but this diminished during testing. In any case, our dependence on animals for food (livestock), companionship (pets), relaxation (horses), and aesthetic value (wildlife) strongly suggests they receive more attention and research regarding the effects of sonic boom exposures.

The effects of sonic booms on aquatic life may not have been investigated to any great extent. This is a result of the initial findings that the attenuation of the sonic

boom in water suggests that these effects should be small (ref. 6). In particular, boom overpressures dissipated to about a tenth of their initial value at a depth of about 60 ft and so appear to pose no threat to aquatic life, including the capacity of fish eggs to hatch. This experience is associated with aircraft traveling at Mach numbers of 3.0 or less. At hypersonic Mach numbers, the aircraft speed can equal or exceed the speed of sound in water (about 4.5 times that in air), thereby greatly increasing the potential penetration of the sonic booms.

Sonic booms produced by aircraft moving at supersonic speeds apply moving loads to the Earth's surface. Although the ground motion recorded was about 100 times the largest natural, steady seismic noise background, it was still less than 1 percent of the accepted seismic damage threshold for residential structures (ref. 6). Experiments have shown that sonic booms probably cannot trigger earthquakes, but they might precipitate incipient avalanches or landslides in exceptional areas which are already stressed to within a few percent of instability. Research efforts on the effects of booms in areas prone to avalanches and landslides have been recommended. Furthermore, the differences between triggering snow and earth avalanches need to be better understood. Once again, the experience thus far is associated with aircraft speeds of Mach number 3.0 or less. The situation may be different at hypersonic speeds.

Questions have been raised concerning the effects of sonic booms on other subsonic aircraft, transport and general aviation types, both in flight and on the ground. Controlled tests (ref. 73) have shown that the sonic-boom-induced accelerations, which were structural rather than rigid body motions, were small relative to those induced by such commonly encountered phenomena as runway roughness and moderate air turbulence. The general conclusions were that sonic booms constitute no serious concern for the safety of all types of subsonic aircraft in flight.

Summary

During flight at supersonic speeds, shock waves are formed which propagate outward in all directions; some may extend to the ground and cause objectionable noise. For vehicles operating at high altitudes, the shock wave patterns coalesce into a bow shock at the front of the vehicle and a tail shock at the rear. The passage of these shock waves past an observer results in rapid changes in atmospheric pressure in the form of an N-wave signature and is interpreted by the ear as two explosive-type sounds, commonly referred to as sonic booms. In a typical supersonic mission the shock waves, which are moving with the aircraft, generate sonic boom "carpets" on the ground whose width depends on flight and atmospheric conditions. These carpets are made up of primary and secondary booms. The primary boom carpet contains the normally observed sonic boom overpressures and results from wave propagation through only that part of the atmosphere below the aircraft. Secondary boom carpets may exist which involve the portion of the atmosphere above the aircraft as well as that below the aircraft. Between the primary and secondary carpets exists a region in which no booms are observed. The secondary boom carpets are more remote from the ground track and the overpressure levels are much less intense than in the primary carpet.

Sonic boom theory, in general, is well established. The evolution of the sonic boom signature from its pattern near the aircraft to the pressure signature received on the ground can be accurately predicted in terms of overpressure level, number and location of shocks, and duration. The complete role of the aircraft configuration in sonic boom generation is embodied in the F-function. Analyses of minimization concepts generally center on calculating F-functions for various configurations. For typical slender supersonic vehicles, the F-function may be computed directly from vehicle geometry via linearized supersonic flow theory. At hypersonic speeds, for which linearized flow theory is not accurate, the problem is that of obtaining the F-function by other means, such as wind tunnel tests or computational fluid dynamics (CFD) codes.

Utilization of the theory of geometric acoustics allows for the inclusion of the real atmosphere and nonlinear steepening on the shock wave system as it propagates to ground. It also allows for the calculation of the number and location of multiple booms resulting from maneuvering flight and the location of "superboom" focal zones. Focus boom signatures can be computed for simple "smooth caustic" foci, but similar results are not yet available for rarer, higher order "superfoci."

A number of sonic boom computer programs have been written. They all perform the same basic calculations, but each has particular capabilities and features added for specific applications. All these programs were originally developed for mainframe computers, but it is expected that personal computer versions will be available.

The primary boom carpet and the disturbances that are experienced within it have been intensely researched. A considerable experimental data base has been accumulated for a wide range of vehicles, Mach numbers, and altitudes. Agreement between measurements and predictions is quite good for both on-track and lateral locations for steady, level flight conditions. Sonic boom overpressures are noted to increase with increasing vehicle size and to decrease with increasing attitude. The lateral extent of the primary boom carpet increases with increasing altitude.

Atmospheric variations, especially those in the first few thousand feet above the Earth's surface, can be very influential in bringing about distortions of the sonic boom signature, changing it from the normally expected N-wave to a "peaked" or "rounded-type" signature. Higher overpressures result when the signatures are peaked, whereas lower overpressures are associated with rounded signatures. This peaking and rounding of the signature is statistical in nature and occurs as a function of either time or distance. As such variations in the sonic boom signature can be expected during routine vehicle operations.

Rapid deviations of a vehicle from steady, level flight can produce considerable modifications in the location, number, and intensity of the ground shock wave patterns. Thus, multiple booms and focused booms may be observed. The pressure buildups in these focus areas are a function of the type maneuver and the accelerations involved and can be 2 to 5 times the nominal levels of steady flight. It is important to note that these focused booms are very localized and do not move with the vehicle. They can be placed to within a few miles of the designated location. Pressure buildup areas associated with turns, pull-up, or pushover maneuvers can be minimized by reducing accelerations. Atmospheric randomness will also decrease or, in some cases, even eliminate focusing altogether.

Secondary sonic booms are quite distinct from primary booms not only in the manner in which they are propagated from the aircraft to the ground but also in

the way their signatures are shaped. For secondary boom signatures, the pressure changes very slowly and is in the subaudible frequency range. This lack of audibility combined with the very low amplitudes makes secondary booms difficult to sense outdoors, but they can be noticeable indoors. The secondary sonic boom carpet and the disturbances experienced within it are not as well-defined as those for the primary boom and only fragmentary observations and measurements are available.

Sonic booms may be minimized through aircraft design and operation. Minimization through design involves modification to the aircraft size, weight, and shape in order to reduce the overpressure or alter the signature waveform. The analytical tools for defining the required aircraft characteristics and means for evaluating trade-offs for boom minimization in terms of aircraft design are available. The most desirable signature shape, from the point of view of minimum response of an outdoor and indoor observer and of structural response, has not yet been established.

Low supersonic "boomless" flight operations are feasible and provide a means for domestic overland flight. The atmosphere plays a significant role in these types of operations, and considerable care must be exercised to assure that the shock waves associated with boomless flights do not extend to the ground. The practicality of such operations is very questionable.

Booms can be observed at ground level from aircraft in steady, level flight at high transonic Mach numbers and relatively low altitudes. The intensity of the boom is substantial because of the very low altitudes, and the signatures are considerably different in nature from the normally observed N-wave associated with fully developed supersonic flow.

The effects of sonic booms (particularly the responses they invoke) are not completely known, even through a considerable data base has been accumulated over the years. Many factors are involved in boom exposure, including the air path, ground path, and building vibrations. Outdoor and indoor stimuli include audible, vibratory, and visual cues. Human response to booms include startle, annoyance, effects on sleep, and long-term effects on health.

Structures reportedly damaged by sonic booms are mostly brittle surfaces and are secondary structural components. The number of damage incidents increases with increasing boom intensity. It may be significant that no damage incidents are reported for boom exposures less than 0.8 lb/ft^2, although the data sample is small.

Sonic booms do not adversely affect human hearing, vision, or circulation. The human psychological response is more complex, involving attitudes and habituation to booms and their sources. Long-term effects on health of repeated daily booms and effects on sleep of repeated night booms are not known Although boom levels of 1.0 lb/ft^2 or greater are apparently unacceptable to a significant portion of the population, a level of acceptability has not been determined.

To date, it has been difficult to make detailed interpretations of the effects of sonic booms on different animal species. Research suggests that boom effects on domestic and wild animals are negligible; however, it is strongly suggested they receive more attention and research.

Since sonic booms attenuate rapidly in water, they appear to pose no threat to aquatic life, nor do they affect the capacity of fish eggs to hatch. At hypersonic Mach numbers, the aircraft speed can equal or exceed the speed of sound in water, thereby greatly increasing the potential penetration of the sonic boom.

Ground motions associated with sonic booms are less than 1 percent of the accepted seismic damage threshold for residential structures. Sonic booms probably cannot trigger earthquakes, but they might precipitate incipient avalanches or landslides in exceptional areas which are already stressed to within a few percent of instability. The situation may be different at hypersonic speeds.

Sonic booms constitute no serious concern for the safety of all types of subsonic aircraft in flight. The boom-induced accelerations are small relative to those induced by runway roughness and moderate air turbulence.

References

1. Proceedings of the Sonic Boom Symposium. *J. Acoust. Soc. America,* vol. 39, no. 5, pt. 2, May 1966, pp. S1–S80.
2. Carlson, Harry W.: Experimental and Analytic Research on Sonic Boom Generation at NASA. *Sonic Boom Research,* A. R. Seebass, ed., NASA SP-147, 1967, pp. 9–23.
3. Garrick, I. Edward: Atmospheric Effects on the Sonic Boom. *Second Conference on Sonic Boom Research,* Ira R. Schwartz, ed., NASA SP-180, 1968, pp. 3–17.
4. Morris, Odell: Experimental Studies of Sonic Boom Phenomena at High Supersonic Mach Numbers *Third Conference on Sonic Boom Research,* Ira R. Schwartz, ed., NASA SP-255, 1970, pp. 193–203.
5. Maglieri, Domenic J.; Carlson, Harry L.; and McLeod, Norman J.: Status of Studies on Sonic Boom. *NASA Aircraft Safety and Operating Problems, Volume I,* NASA SP-270, 1971, pp. 439–456.
6. Ribner, H. S.; and Hubbard, H. H., eds.: *Proceedings of the Second Sonic Boom Symposium.* American Inst. of Physics, 1972.
7. Hubbard, Harvey H.; Maglieri, Domenic J.; and Stephens, David G.: *Sonic-Boom Research—Selected Bibliography With Annotation.* NASA TM-87685, 1986.
8. *Civil Aircraft Sonic Boom.* Aeronautics and Space, Code of Federal Regulations, Title 14, Part 91, Federal Aviation Adm., Jan. 1, 1987, pp. 169–170.
9. National Sonic Boom Evaluation Off.: *Sonic Boom Experiments at Edwards Air Force Base.* NSBEO-1-67 (Contract AF 49(638)-1758), Stanford Research Inst., July 28, 1967.
10. Gardner, John H.; and Rogers, Peter H.: *Thermospheric Propagation of Sonic Booms From the Concorde Supersonic Transport.* NRL Memo. Rep. 3904, U.S. Navy, Feb. 14, 1979. (Available from DTIC as AD A067 201.)
11. George A. R.; and Kim, Y. N.: High-Altitude Long-Range Sonic Boom Propagation. *J. Aircr.,* vol. 16, no. 9, Sept. 1979, pp. 637–639.
12. Balachandran, Nambath K.; Donn, William L.; and Rind, David H.: Concorde Sonic Booms as an Atmospheric Probe. *Science,* vol. 197, no. 4298, July 1, 1977, pp. 47–49.
13. Donn, William L.: Exploring the Atmosphere With Sonic Booms. *American Sci.,* vol. 66, no. 6, Nov.–Dec. 1978, pp. 724–733.
14. Liszka, Ludwik: Long-Distance Focusing of Concorde Sonic Boom. *J. Acoust Soc. America,* vol. 64, no. 2, Aug. 1978, pp. 631–635.
15. [illegible] Edward J.; and Pierce, Allan D.: *Detection and Assessment of Secondary Sonic Booms in New [illegible].* FAA AEE-80-22, May 1980.
16. Whitham, G. B.: The Flow Pattern of a Supersonic Projectile. *Commun. Pure & Appl. Math.,* vol. V, no. 3, Aug. 1952, pp. 301–348.
17. Hayes, Wallace D.: *Linearized Supersonic Flow.* Ph.D. Thesis, California Inst. of Technology, 1947.
18. Hayes, Wallace D.: Brief Review of the Basic Theory. *Sonic Boom Research,* A. R. Seebass, ed., NASA SP-147, 1967, pp. 3–7.
19. Lomax, Harvard: *The Wave Drag of Arbitrary Configurations in Linearized Flow as Determined by Areas and Forces in Oblique Planes.* NACA RM A55A18, 1955.
20. Walkden, F.: The Shock Pattern of a Wing-Body Combination, Far From the Flight Path. *Aeronaut. Q.,* vol. IX, pt. 2, May 1958, pp. 164–194.
21. Whitham, G. B.: On the Propagation of Weak Shock Waves. *J. Fluid Mech.,* vol. 1, pt. 3, Sept. 1956, pp. 290–318.
22. Seebass, R.: Sonic Boom Theory. *J. Aircr.,* vol. 6, no. 3, May–June 1969, pp. 177–184.
23. Landau, L.: On Shock Waves at Large Distances From the Place of Their Origin. *J. Phys. USSR,* vol. 9, no. 6, 1945, pp. 496–500.

24. DuMond, Jesse W. M.; Cohen, E. Richard; Panofsky, W. K. H.; and Deeds, Edward: A Determination of the Wave Forms and Laws of Propagation and Dissipation of Ballistic Shock Waves. *J. Acoust. Soc. America*, vol. 18, no. 1, July 1946, pp. 97–118.
25. Hayes, Wallace D.; Haefeli, Rudolph C.; and Kulsrud, H. E.: *Sonic Boom Propagation in a Stratified Atmosphere, With Computer Program.* NASA CR-1299, 1969.
26. George, A. R.; and Plotkin, Kenneth J.: Sonic Boom Waveforms and Amplitudes in a Real Atmosphere. *AIAA J.*, vol. 7, no. 10, Oct. 1969, pp. 1978–1981.
27. Maglieri, Domenic J.; and Carlson, Harry W.: *The Shock-Wave Noise Problem of Supersonic Aircraft in Steady Flight.* NASA MEMO 3-4-59L, 1959.
28. Blokhintzev, D. I.: *Acoustics of a Nonhomogeneous Moving Medium.* NACA TM 1399, 1956.
29. Officer, C. B.: *Introduction to the Theory of Sound Transmission With Application to the Ocean.* McGraw-Hill Book Co., Inc., c.1958.
30. Keller, J. B.: Geometrical Acoustics. I. The Theory of Weak Shock Waves. *J. Appl. Phys.*, vol. 25, no. 8, Aug. 1954, pp. 938–947.
31. Thomas, Charles L.: *Extrapolation of Sonic Boom Pressure Signatures by the Waveform Parameter Method.* NASA TN D-6832, 1972.
32. Plotkin, K. J.; and Cantril, J. M.: Prediction of Sonic Boom at a Focus. AIAA Paper 76-2, Jan. 1976.
33. Haber, Jerold M.; and Drake, James F.: *Sonic Boom Risk Management: SABER & SABERPLOT User's Manual.* Contract No. F04703-79-C-0004, Task No. 10/79-16, J. H. Wiggins Co., July 15, 1980.
34. Taylor, Albion D.: *The Traps Sonic Boom Program.* NOAA Tech. Memo. ERL ARL-87, U.S. Dep. of Commerce, July 1980.
35. Plotkin, Kenneth J.: *Sonic Boom Focus Conditions Due to Tactical Air Operations.* WR 84-8, Wyle Lab. Feb. 1984.
36. Carlson, Harry W.: *Simplified Sonic-Boom Prediction.* NASA TP-1122, 1978.
37. Guiraud, Jean-Pierre: Acoustique Geometrique, Bruit Balistique des Avions Supersoniques et Focalisation. *J. Mech*, vol. 4, no. 2, June 1965, pp. 215–267.
38. Gill, Peter M.; and Seebass, A. Richard: Nonlinear Acoustic Behavior at a Caustic: An Approximate Analytical Solution. *Aeroacoustics: Fan, STOL, and Boundary Layer Noise; Sonic Boom; Aeroacoustic Instrumentation,* Henry T. Nagamatsu, ed., American Inst. of Aeronautics and Astronautics, c.1975, pp. 353–386.
39. Gill, Peter Maxwell: *Nonlinear Acoustic Behavior at a Caustic.* Ph.D. Thesis, Cornell Univ., 1974.
40. Fung, K.-Y.: Shock Wave Formation at a Caustic. *SIAM J. Appl. Math.*, vol. 39, no. 2, Oct. 1980, pp. 355–371.
41. Plotkin, Kenneth J.: *Focus Boom Footprints for Various Air Force Supersonic Operations.* WR 85-22, Wyle Lab., Oct. 1985.
42. Haglund, George T.; and Kane, Edward J.: *Analysis of Sonic Boom Measurements Near Shock Wave Extremities for Flight Near Mach 1.0 and for Airplane Accelerations.* NASA CR-2417, 1974.
43. Wanner, Jean-Claude L.; Vallee, Jacques; Vivier, Claude; and Thery, Claude: Theoretical and Experimental Studies of the Focus of Sonic Booms. *J. Acoust. Soc. America*, vol. 52, no. 1, pt. 1, July 1972, pp. 13–32.
44. Plotkin, Kenneth J.: *Evaluation of a Sonic Boom Focal Zone Prediction Model.* WR 84-43, Wyle Lab., Feb. 1985.
45. Cramer, M. S.; and Seebass, A. R.: Focusing of Weak Shock Waves at an Arête. *J. Fluid Mech.*, vol. 88, pt. 2, Sept. 27, 1978, pp. 209–222.
46. Cramer, M. S.: Focusing of a Weak Three-Dimensional Shock Wave. *AIAA J.*, vol. 19, no. 10, Oct. 1981, pp. 1363–1365.
47. Hicks, Raymond M.; Mendoza, Joel P.; and Thomas, Charles L.: *Pressure Signatures for the Apollo Command Module and the Saturn V Launch Vehicle With a Discussion of Strong Shock Extrapolation Procedures.* NASA TM X-62,117, 1972.
48. Ashby, George C., Jr.: *Near-Field Sonic-Boom Pressure Signatures for the Space Shuttle Launch and Orbiter Vehicles at Mach 6.* NASA TP-1405, 1979.
49. Ashby, George C., Jr.: *A Study of the Sonic-Boom Characteristics of a Blunt Body at a Mach Number of 6.* NASA TP-1787, 1980.
50. Tiegerman, B.: *Sonic Booms of Drag Dominated Hypersonic Vehicles.* Ph.D. Thesis, Cornell Univ., 1975.
51. Seebass, A. Richard: *Hypersonic Boom.* Tech. Commun. 030, Flight Sciences Lab., Boeing Scientific Research Lab., June 1970.

52. Seebass, A. R.; and George, A. R.: Design and Operation of Aircraft To Minimize Their Sonic Boom. *J. Aircr.*, vol. 11, no. 9, Sept. 1974, pp. 509–517.
53. Henderson, Herbert R.; and Hilton, David A.: *Sonic-Boom Measurements in the Focus Region During the Ascent of Apollo 17.* NASA TN D-7806, 1974.
54. Garcia, Frank, Jr.; Jones, Jess H.; and Henderson, Herbert R.: A Comparison of Measured and Theoretical Predictions for STS Ascent and Entry Sonic Booms. *Shuttle Performance: Lessons Learned, Part 2,* James P. Arrington and Jim J. Jones, compilers, NASA CP-2283, Pt. 2, 1983, pp. 1277–1301.
55. Cotten, Donald; and Donn, William L.: Sound From Apollo Rockets in Space. *Science,* vol. 171, no. 3971, Feb. 12, 1971, pp 565–567.
56. Plotkin, Kenneth J.; and George, A. R.: Propagation of Weak Shock Waves Through Turbulence. *J. Fluid Mech.,* vol. 54, pt. 3, Aug. 8, 1972, pp. 449–467.
57. Maglieri, Domenic J.; and Lansing, Donald L.: *Sonic Booms From Aircraft in Maneuvers.* NASA TN D-2370, 1964.
58. *NRL Investigations of East Coast Acoustics Events 2 December 1977—15 February 1978.* Dep. of Navy, Mar. 10, 1978.
59. Seebass, R.: Minimum Sonic Boom Shock Strengths and Overpressures. *Nature,* vol. 221, no. 5181, Feb. 15, 1969, pp. 651–653.
60. Jones, L. B.: Lower Bounds for Sonic Bangs in the Far Field. *Aeronaut. Q.,* vol. XVIII, pt. 1, Feb. 1967, pp. 1–21.
61. Jones, L. B.: Lower Bounds for the Pressure Jump of the Bow Shock of a Supersonic Transport. *Aeronaut. Q.,* vol. XXI, pt. 1, Feb. 1970, pp. 1–17.
62. Mack, R. J.; and Darden, C. M.: Some Effects of Applying Sonic Boom Minimization to Supersonic Cruise Aircraft Design. *J. Aircr.,* vol. 17, no. 3, Mar. 1980, pp. 182–186.
63. Niedzwiecki, A.; and Ribner, H. S.: Subjective Loudness of N-Wave Sonic Booms. *J. Acoust. Soc. America,* vol. 64, no. 6, Dec. 1978, pp. 1617–1621.
64. Niedzwiecki, A.; and Ribner, H. S.: Subjective Loudness of "Minimized" Sonic Boom Waveforms. *J. Acoust. Soc. America.* vol. 64, no. 6, Dec. 1978, pp. 1622–1626.
65. Cheng, D. H.; and Benveniste, J. E.: Transient Response of Structural Elements to Traveling Pressure Waves of Arbitrary Shape. *Int. J. Mech. Sci.,* vol. 8, no. 10, Oct. 1966, pp. 607–618.
66. McLean, F. Edward; Carlson, Harry W.; and Hunton, Lynn W.: *Sonic-Boom Characteristics of Proposed Supersonic and Hypersonic Airplanes.* NASA TN D-3587, 1966.
67. Miller, David S.; and Carlson, Harry W.: *A Study of the Application of Heat or Force Fields to the Sonic-Boom-Minimization Problem.* NASA TN D-5582, 1969.
68. Driver, Cornelius; and Maglieri, Domenic J.: The Impact of Emerging Technologies on an Advanced Supersonic Transport. *ICAS Proceedings, 1986—15th Congress of the International Council of the Aeronautical Sciences,* P. Santini and R. Staufenbiel, eds., International Council of Aeronautical Sciences, c.1986, pp. 213–220. (Available as ICAS-86-2.2.3.)
69. Vapor Condensation Makes F-14 Shockwaves Visible. *Aviation Week & Space Technol.,* vol. 107, no. 21, Nov. 21, 1977, pp. 46–47.
70. Hubbard, Harvey H.; and Mayes, William H.: Sonic Boom Effects on People and Structures. *Sonic Boom Research,* A. R. Seebass, ed., NASA SP-147, 1967, pp. 65–76.
71. ARDE Assoc.: *Response of Structures to Aircraft Generated Shock Waves.* WADC Tech. Rep. 58-169, U.S. Air Force, Apr. 1959. (Available from DTIC as AD 229 463L.)
72. Sutherland, Louis C.: *Low Frequency Response of Structures.* WR 82-18, Wyle Lab., May 1982.
73. Maglieri, Domenic J.; and Morris, Garland J.: *Measurements of the Response of Two Light Airplanes to Sonic Booms.* NASA TN D-1941, 1963.